RADIAL BASIS FUNCTION MODEL OF NAVIER-STOKES EQUATIONS FOR WATER WAVES

by

Yavuz Tokmak

B.S., in Civil Engineering, Boğazici University, 2002

M.S., in Civil Engineering, Boğazici University, 2005

Submitted to the Institute for Graduate Studies in
Science and Engineering in partial fulfillment of
the requirements for the degree of
Doctor of Philosophy

Graduate Program in Civil Engineering

Boğaziçi University

2018

RADIAL BASIS FUNCTION MODEL OF NAVIER-STOKES EQUATIONS FOR WATER WAVES

APPROVED BY:

Assoc. Prof. Osman BÖREKÇİ (Thesis Supervisor)	.....
Prof. Cem AVCI	.....
Prof. Serdar BEJİ	.....
Prof. Yasin FAHJAN	.....
Assoc. Prof. Emre OTAY	.....

DATE OF APPROVAL: 04.06.2018

ACKNOWLEDGEMENTS

I would like to express my sincere gratitude to Dr. Börekçi for his patience above all and for his guidance, motivation and fatherly attitude. I owe the completion of this study to his limitless understanding on the circumstances a scholar may face throughout an advanced study.

Also, I am indebted to Dr. Luş for his vision and rejecting my ex-matriculation request by turning a breaking point in my life into a milestone. I would not have the chance to rewrite the model of this study and submit for approval otherwise.

I would like to thank the members of my thesis committee Dr. Avci, Dr. Otay, Dr. Fahjan, Dr. Beji and Dr. Güngör for their time, support and guidance throughout the review of this document. And, I am grateful to Dr. Kılıç for sharing his computer resources during the simulations.

Finally I would like to thank my mother and grandmother who gave me the inspiration to rewrite the model of this study.

ABSTRACT

RADIAL BASIS FUNCTION MODEL OF NAVIER-STOKES EQUATIONS FOR WATER WAVES

In this study a numerical model using the radial basis function collocation method (RBFCM) is developed for water wave propagation described by the Navier-Stokes equations. For the test cases, two dimensional horizontal bottom tests and submerged breakwater test are performed and the results are verified with the expected solutions and the experiment results of Luth et al. (1994). The collocation configuration is implemented to change instantly depending on the evolution of the free surface so that a center close to the surface below a crest can be out of the defined collocation set at another instant if there is trough on the free surface. The projection method of Chorin (1968) is used to create an auxiliary equation from the continuity to compute for the pressure in the flow field and the resulting Poisson equation is modeled using the collocation on the boundary technique to obtain better accuracy with the definition of additional out of domain centers close to the boundary which makes it possible to define the governing equation as well as the boundary condition at a boundary collocation center. The model is developed using the advanced features provided by the recent programming languages so that it is extensible to account for more details in the flow field and also different solvers can be implemented for different type of flows and problems.

ÖZET

SU DALGALARI İÇİN NAVİER-STOKES DENKLEMLERİNİN RADYAL BAZLI FONKSİYON MODELİ

Bu çalışmada, Navier-Stokes denklemleriyle tarif edilen dalga ilerlemesi problemi için radyal bazlı kolokasyon yöntemini kullanan bir sayısal model geliştirilmiştir. Testi için iki boyutlu yatay taban tesleri ve batık dalgakıran testi yapılmıştır ve sonuçlar beklenen çözümler ile ve Luth et al. (1994) deney sonuçlarıyla doğrulanmıştır. Kolokasyon tertibi zaman içinde değişecek şekilde tatbik edilerek yüzeyin durumuna göre tepe altında yüzeye yakın bir kolokasyon merkezinin başka bir çözüm anında yüzeyde çukur olması ihtimalinde çözüm alanında bulunan geçerli kolkasyon kümesi dışında kalması sağlanmıştır. Süreklilik denkleminden yedek bir denklem yaratarak basınç alanını çözmek için Chorin (1968) projeksiyon yöntemi kullanışmıştır ve sonunda elde edilen Poisson denklemi sınırda kolokasyon yöntemiyle modellenerek çözüm alanı dışında sınıra yakın konumlara yerleştirilen kolokasyon merkezleri sayesinde bir sınır merkezinde aynı anda çözüm alanında geçerli denklemi ve sınır şartını sağlamak mümkün olmuştur. Model programlama dillerinin güncel ileri özellikleriyle geliştirilerek akış alanında daha çok detayı açıklayabilecek uzantıların yapılmasına ve aynı zamanda başka çözücüler yazarak başka tür akıntıların çözülmesine olanak vermektedir.

TABLE OF CONTENTS

LIST OF FIGURES

LIST OF TABLES

LIST OF SYMBOLS

a	Wave amplitude
B_j	j-th stream function coefficient
c	Shape parameter
C	Wave celerity
C^m	m-th order complex domain
C_n	Estimate of Sommerfeld's radiation boundary condition constant at the n-th location
d	Local depth
g	Gravitational acceleration
f	Derivative function
H	Wave height
k	Wave number
k_i	i-th Runge-Kutta coefficient
L	Wave length
N	Number of centers
p	Pressure per unit density
p_t	Total pressure per unit density
r	Radial distance between two centers
t	Time variable
t_0	Time at the start of a simulation
u	Horizontal velocity component
u^*	Predicted horizontal velocity component
$\tilde{u}$	Mean fluid velocity
u_s	Horizontal velocity component on the free surface
U_R	Ursell Parameter
x	Horizontal coordinate
$\mathbf{x}$	Coordinate vector
$\mathbf{x_j}$	Coordinate vector at center j
w	Vertical velocity component

w^*	Predicted vertical velocity component
w_1	Sponge layer damping term coefficient
w_2	Sponge layer damping term coefficient
w_s	Vertical velocity component on the free surface
z	Vertical coordinate
z_b	Bottom coordinate
α	Interpolation constant
Δt	Incremental time
ϵ	Stokes perturbation parameter
η	Free Surface Parameter
η_0	Free Surface Parameter at time $t = t_0$
ν	Kinematic viscosity
σ	Normalized vertical coordinate
φ	Radial basis function
ψ	Stream function
ϕ	Velocity potential function

LIST OF ACRONYMS/ABBREVIATIONS

2D	Two Dimensional
3D	Three Dimensional
ABM2	Adams-Bashforth-Moulton
ABP	Adams-Bashforth Predictor
AMC	Adams-Moulton Corrector
ALE	Arbitrary Lagrangian-Eulerian
DFSBC	Dynamic Free Surface Boundary Condition
GARBF	Gaussian Radial Basis Function
IMQRBF	Inverse Multiquadric Radial Basis Function
IQRBF	Inverse Quadric Radial Basis Function
KdV	Korteweg-deVries
KFSBC	Kinematic Free Surface Boundary Condition
LES	Large Eddy Simulation
LSM	Level Set Method
MAC	Marker and Cell
MFS	Method of Fundamental Solutions
MQ	Multiquadric
MQRBF	Multiquadric Radial Basis Function
NS	Navier Stokes
NSWE	Nonlinear Shallow Water Equation
PDE	Partial Differential Equation
PISO	Pressure Implicit with Splitting of Operators
RANS	Reynolds Averaged Navier Stokes
RBC	Radiation Boundary Condition
RBF	Radial Basis Function
RBF-FD	Radial Basis Function-Finite Differences
RBFCM	Radial Basis Function Collocation Method
SIMPLE	Semi-Implicit Method for Pressure-Linked Equations

SIMPLEC	Semi-Implicit Method for Pressure-Linked Equations Consistent
SIMPLER	Semi-Implicit Method for Pressure-Linked Equations Revised
SPH	Smooth Particle Hydrodynamics
TPS	Thin Plate Spline
VOF	Volume of Fluid

1. INTRODUCTION

Mostly generated by the winds blowing over large ocean or sea surfaces, water wave motion is an important phenomenon that needs careful consideration because accurate prediction of the wave parameters plays a crucial role in the design of coastal or off-shore structures and in the solution of the engineering problems occurring at the nearshore region.

Several methodologies have been developed to measure the wave parameters that can be broadly classified as physical and non-physical. Physical methods are mainly composed of laboratory and field studies where data collection is performed to extract information about the waves. On the other hand, mathematical modeling, which is not exactly an alternative but rather a complementary work, is used estimate the wave parameters. With the help of these non-physical models, a deeper understanding of the problem is aimed to be developed. Also, measured physical data or experimental results are used for the verification of the mathematical models.

Within the scope of laboratory tests, real physics of the problems related to the the wave motion are simulated at certain scales. A wide variety of simulations are available from those focused on pure wave mechanics to interaction of the waves with their environment. On the other hand, wave parameters are measured and recorded in field observations. This can be achieved by special instruments located at fixed on-site or remote stations or attached to moving bodies like vessels.

Mathematical modeling of waves is mainly based on mathematical descriptions of the wave motion made by making use of the physical laws under certain assumptions. Once a set of equations are constructed for the physics of the problem, exact or numerical solutions are sought by using some modeling methods which are analytical, numerical or statistical. Any combinations of these methods are also possible depending on the approach taken. It has to be noted at this point that a mathematical model is as good as the physics built into the model.

Of these methods, statistical approach does not always need determinate mathematical equations of the wave motion and generally relies on data over which predictions are made through some set of relations or distributions. Similar to stochastic models, spectral models have also been developed assuming waves are not monochromatic and water surface is composed of waves with different frequencies and directions. Since, this study is about the propagation of monochromatic waves with a determinate physics, stochastic and spectral models are not discussed further.

On the other hand, analytical and numerical methods propose solutions to the determinate description of the wave motion under certain assumptions. Initial method provides exact solutions, and the latter provides approximate solutions.

Analytical solution development of the wave models dates back to the early days of research on the topic, as it was the only tool at that time. However with the invention of computers, numerical models have started to be developed, and in parallel to the enormous increase in the processing power of computers, numerical models have gained priority. This is not only because analytical solutions are applicable to more particular cases but also it has become possible to account for different aspects of the problems in the same model through coupling multiple physics together. In this way, limitations to analytical solutions have been breached and the needs of the industry and research field have been met in a broader spectrum. A numerical method typically includes the following steps.

(i) Discretization of the continuous problem domain.
(ii) Proposition of an approximate definition with undetermined coefficients for the unknowns of the problem.
(iii) Construction of a set of equations on the discrete domain based on the mathematical description of the problem.
(iv) Imposition of the initial and boundary conditions.

Approximate solutions to the problem variables are found by computing the undetermined coefficients. Meanwhile, several numerical techniques are employed depending

on the linear or nonlinear nature of the problem.

Every numerical method has its own way of constructing the set of equations on how the problem domain is discretized and the approximate solution is proposed. A general distinction can be made among them through the definition of approximate solutions whether a local portion of the discretized domain is used or not.

Models with local definitions of the unknowns are called local methods whereas the models with definitions that are using the information of the whole domain are called global methods. On the other hand, numerical methods differ according to the geometrical elements they use to discretize the problem domain. Through the definition of discrete elements or simply points, the models end up in different sets of equations.

One of the most difficult aspects of geometry discretization occurs when the problem domain deforms in time. This is always the case with the wave propagation models where the free surface changes in time and the free surface boundary conditions are to be satisfied on this deforming boundary. And, since some methods use geometrical elements that do not change in time, they need special treatment to account for the domain deformation in the resulting set of equations. This may result in a pay-off from the accuracy and bring an inevitable difficulty in the development phase.

Likewise, it may be difficult for a method to define some of the parameters due to the restrictions imposed by its geometrical elements. In such models, for example, a set of parameters are computed at certain locations of the element while some other parameters are located and computed elsewhere. This might cause loss of generality and accuracy. For example, in a flow field with the pressure and the velocity field are the main unknowns, some models might have elements where the pressure field is computed on the surface while the velocity field is computed in the middle of these elements.

Therefore numerical models that are made up of a mathematical model and a numerical implementation of it, can be evaluated according their **applicability**, **com-**

plexity, **accuracy** and **performance**. It is always desired from a numerical model to be applicable to a wide range of problems and contain as much complexity as possible so that special treatments are not required. In addition, the results are desired to be at the highest level of accuracy and to use least computer resources in order to obtain the results as fast as possible.

In this study a numerical model is developed based on the Navier Stokes (NS) equations using the radial basis function collation method (RBFCM). By the selection of NS Equations it is aimed to develop a numerical model with a mathematical formulation that has less limitations and assumptions compared to other models. In this sense, NS Equations are applicable to any kind of flow problems without any restrictions, although it is limited by other factors such as the limits of the computational power of modern computers.

It has to be noted at this point that as the waves approach the shore, at some point waves start to overturn and breaking occurs most of the time and there are various types of mechanisms that need to be identified during breaking. These mechanisms are needed to be implemented in a model if wave breaking is desired to be accounted for. Therefore the model developed in this study must be clearly identified that wave propagation is modeled up to the breaking point.

RBFCM is selected because it is it is easy to track the surface deformation since position of the radial basis function (RBF) centers and collocation nodes can change in time. Moreover, since it is easy to express geometrical features, less modeling efforts needed for RBFCMs compared to alternative methods. Also, flexibility in the expression of geometry makes it possible to define the parameters exactly compared to methods that needs mostly inexact definitions

In this study, problem domain is reduced into a two-dimensional (2D) vertical plane to speed up computations sacrificing the ability to validate the diffraction and refraction effects on water waves occurring due to a variable bottom topography. However, the model can be extended into three dimensions (3D) without much effort due

to the flexibility of RBFCM.

Viscosity is taken constant as it is deemed satisfactory for the purposes of this study and assumed that any rotational effects originating at the bottom boundary do not have enough time to develop inside flow region. This makes it possible to ignore turbulent effects. However, a turbulence model can easily be coupled with NS Equations.

Verification of the model is done by performing two types of numerical tests. In the first type, input wave defined on the influx boundary is propagated on an horizontal bottom where it is expected to propagate downstream without any change in its phase and amplitude. In the second type, submerged breakwater laboratory test results of Luth et al. (1994) are regenerated. It is found that the simulation results are in good agreement with the solutions or laboratory test results.

In the following chapter, a literature review of the topic is given. In the first part, some of the mathematical and numerical water wave models present in the literature are presented. In the second part of the chapter, a brief review on RBFs and RBFCM is given.

In Chapter 3, mathematical model is introduced. The governing NS equations are presented along with the problem geometry and the boundary and initial conditions. Also, assumptions and limitations of the model are listed.

Chapter 4 is about the numerical methodology followed in the study, namely the RBFCM. Definition of the unknowns with the undetermined coefficients are given according to RBFCM. It is shown how the continuous problem geometry is handled by discrete set of RBF centers. Numerical formulation of the boundary conditions and their implementation in the model are presented. Also, time marching methods used in the model are given in detail.

In the last two chapters, test results are presented and conclusion of the study is

given.

2. LITERATURE REVIEW

2.1. Introduction

There have been numerous studies for the wave propagation problem present in the literature. While the early models use analytical techniques, with the invention of computers, numerical techniques have been started to be applied by researchers and engineers. Computers have lead to substantial advancement in the state-of-the-art of water wave propagation modeling and have made it possible to develop alternative models mostly with a deeper understanding and knowledge. And, it can be clearly seen that the capacity and capability of the models have been improved in parallel to the advancement in computer technology. Also, while recent models are more sophisticated than their predecessors, they require more computer resources.

As it was stated before, only determinate models for monochromatic waves are reviewed. Stochastic and spectral models are omitted.

A clear distinction of the wave models presented below is tried to be avoided because a model is characterized with many aspects and it is natural that some of these make a clear distinction, some other aspect overlap. Therefore, they are rather given in groups or separately. Some models have limitations with respect to the water depth and it can be seen that efforts have been made to extend their validity and applicability. NS Equation models, on the other hand, are valid for all depths without any limitations.

A detailed discussion on small amplitude and shallow water models can be found in the texts such as Stoker (1957), Le Méhauté (1976), Dean and Dalrymple (1984), Sobey *et al.* (1987), Kowalik and Murty (1993), Dingemans (1997a,b), Svendsen (2006) and Whitham (1999).

After the review of the wave models, a brief review is given on the RBFCM which

is a more recent numerical technique compared to alternative methods. Also, various RBFs used for the solution of partial differential equations (PDEs) are introduced and development of the method is reviewed.

2.2. Small Amplitude Wave Model and Finite Amplitude Extension Models

2.2.1. Linear Wave Model

The linear wave solution to the wave motion problem was first proposed by Airy (1845). This model is alternatively called the linear wave, small amplitude wave or Airy wave. Wave height (H) or wave amplitude (a) is very small compared to wave length and local depth(d). In other words, wave steepness (H/L), relative wave height (H/d) are assumed to be very small, i.e. $H/L << 1$, $H/d << 1$. This implies that the free surface can be accepted at the mean water level when the free surface boundary conditions are imposed.

As a wave approaches to the shore, its wave height increases because of shoaling and its wave length decreases. In the mean time, local depth becomes smaller. Therefore, wave steepness and relative wave height increases and assumptions of linear wave model is violated and thus its validity breaks.

Another parameter that can be classify the wave models valid within a limited range is the Ursell number given in Ursell (1953). Its form applicable to small amplitude and shallow water waves is as follows.

$$U_R = \frac{H}{L}\left(\frac{L}{d}\right)^3 \tag{2.1}$$

where U_R is the Ursell number. Following from the very small definition of wave steepness and wave length-to-depth ratio described above, Ursell parameter is very small ($U_R << 1$) for linear waves. In Table 2.1 several properties of the Airy Wave model are listed. Although a comparison of the wave models with limited nature are

Table 2.1. Airy Wave Model Properties

Wave Theory	Linear (Airy) Wave
Characteristic Parameters	$H/d << 1$, $H/L << 1$, $U_R << 1$
Range of Validity	Deep Water ($d/L > 0.5$)
	Intermediate Water ($0.05 < d/L < 0.5$)
Assumptions	Irrotational, Nonhydrostatic, Perfect fluid,
	Oscillatory, Exact solution, 2D vertical domain,
	Flat impermeable bottom, Negligible surface tension

given later, it must be noted here that Airy wave theory gives reasonable results at intermediate water depths while fair results are obtainable in deep water. The results deteriorate in shallow water.

Analytical solutions can be obtained by assuming that a velocity field is derivable from a potential function $\phi(x, z, t)$ where x is the horizontal and z the vertical direction. This means the solutions are valid on a 2D vertical domain where the third dimension is omitted with the assumption that wave crests are long enough and wave properties do not change in the transverse direction. Also, the fluid is ideal for Airy models so that friction is not considered.

2.2.2. Stokes Wave Model

Theory of Stokes Waves is found in Stokes (1847) where linear Airy wave theory is extended by defining a perturbation parameter of a series solution. This makes it possible to include nonlinear terms in the solution of the wave problem and get better results compared to linear waves that are equivalent to the results obtained by selecting only the order one expansion term. It is shown that it is possible to develop a wave model at any order with the perturbation method implemented in the process of deriving solutions.

Table 2.2. Stokes Wave Model Properties

Wave Theory	Stokes Waves
Characteristic Parameters	$H/d << 1$, $H/L << 1$, $U_R < 10$
Range of Validity	Deep Water ($d/L > 0.5$)
	Intermediate Water ($0.05 < d/L < 0.5$)
	Shallow Water (limited) ($d/L < 0.05$)
Assumptions	Irrotational, Nonhydrostatic, Perfect fluid,
	Oscillatory, Power series in H/L, 2D vertical domain,
	Flat impermeable bottom, Negligible surface tension

In the case when small wave steepness ($H/L << 1$) assumption is valid, there is only one mode of the solution and the wave form is purely sinusoidal. However, for a more general case, small wave steepness assumption is neglected and the expansion parameter $\epsilon = 2\pi H/L$ is assumed as an order 1 ($O(1)$) quantity. This way powers of ϵ becomes meaningful and a wave model to any order can be generated. In particular, the first order Stokes wave is the equivalent of linear wave model.

Fenton (1985) derived fifth order Stokes waves that are valid from deep water to shallow water. However, it must be noted that validity remains as long as the wave steepness is in similar order to the order of the Stokes waves. Otherwise, for long waves in shallower region of the ocean, wave steepness might become very small and thus Stokes solutions become invalid. In that case, alternative solutions are available in the literature and reviewed in Section 2.3.

Properties of Stokes wave model is summarized in Table 2.2. The main difference from the linear wave theory is in the conditions used for the validity of the wave and the nature of the solution since the solution is exact for the linear waves whereas it is a power series expression for Stokes waves.

2.2.3. Stream Function Wave Model

Although there have been efforts to derive the Stokes waves in higher orders for more accuracy and extending the validity region, the derivation process becomes difficult manually after the second order. Therefore, following the work Chappelear (1961) in which a numerical solution to the wave propagation problem is proposed, Dean (1965) uses the stream function equation as the governing equation valid on a problem domain, formulates the flow field variable, namely the stream function using a series and in the least square sense obtained the coefficients of this series by best fitting the so-called dynamic free surface boundary condition (DFSBC).

Method of Dean (1965) is simpler than that of Chappelear (1961) and these two studies are the first models using power of computers in water wave propagation problems. Also, the results of 40 wave cases are tabulated in Dean (1974) to be used without the need of a computer.

Rienecker and Fenton (1981) uses a simpler method to obtain the Fourier series coefficients but it is not applicable to deep water waves. Therefore Fenton (1988) modifies this method so that coefficients are obtainable both for deep water and finite depth region. A computer program is also given in the study.

In general these models are called the Fourier approximation methods since the coefficients of the Fourier series are computed numerically. Also, along with the Stokes waves where the parameters are expressed by a Fourier series, stream function method can also be classified as Fourier method.

Although approximate, results of the stream function wave model are superior to the Stokes waves used in the studies present in the literature. This is because computers that have made it possible to propose a solution to any order. And, it has to be noted that the limited capability of Stokes waves in shallow water is also surpassed by stream functions up to 20th order.

Table 2.3. Stream Function Wave Model Properties

Wave Theory	Stream Function Waves
Characteristic Parameters	None
Range of Validity	Deep Water ($d/L > 0.5$)
	Intermediate Water ($0.05 < d/L < 0.5$)
	Shallow Water ($d/L < 0.05$)
Assumptions	Irrotational, Nonhydrostatic, Perfect fluid,
	Oscillatory, Fourier series in d/L,
	2D vertical domain, Exact,
	Flat impermeable bottom, Negligible surface tension

In Table 2.3 stream function wave properties are listed. Since it is a numerical model and wave properties can be computed to any order, theoretically there is no characteristic parameter limiting the validity of the theory except the breaking limit of the waves.

2.3. Shallow Water Models

Expansion parameter of the Stokes Waves, $\epsilon = 2\pi H/L$, is also an order 1 ($O(1)$) quantity. However, in shallow water, long wave length, L, is much higher than the local depth d that the assumption on the expansion parameter becomes invalid as it violates being an order 1 quantity.

In Ursell (1953), linear shallow water waves are classified according to Ursell number where its value is much less than one ($U_R << 1$), while it is an order one quantity ($U_R \sim O(1)$) for cnoidal and solitary waves and much higher than one ($U_R >> 1$) for nonlinear shallow water waves.

Table 2.4. Linear Shallow Water Wave Model Properties

Wave Theory	Linear Shallow Water Waves
Characteristic Parameters	$H/d << 1$, $U_R << 1$
Range of Validity	Shallow Water ($d/L < 0.05$)
Assumptions	Irrotational, Hydrostatic, Perfect fluid,
	Oscillatory, Fourier series in d/L, 2D horizontal domain,
	Varying impermeable bottom, Negligible surface tension

2.3.1. Linear Shallow Water Wave Models

Neglecting the convective terms, inertia, friction and nonlinear terms in the mometum and continuity equations linear shallow water wave equations can be obtained. With their application to several different cases under the assumptions $H/d << 1$ and $U_R << 1$, exact solutions can be obtained for this model. Due to these assumptions, these waves are called as long waves of small amplitude.

For the properties listed Table 2.4, it must be noted that the pressure in hydrostatic and solutions for various bathymetries exist for linear shallow water wave equations. Although, it is always possible to obtain numerical solutions using linear shallow water equations and various treatments can be introduced into the models for computation of the different aspects of the waves, only exact solutions are considered in the table.

2.3.2. Cnoidal, Solitary and Boussinesq Wave Models

For order one ($O(1)$) Ursell numbers, U_R, it is possible to obtain the Boussinesq equations by using a partial solution solution of the Laplace equation in the kinematic (KFSBC) and dynamic free surface boundary conditions. This partial solution in terms of velocity potential is obtained using the bottom velocity potential and it displays the

variation of potential along the vertical direction.

While application of KFSBC results in a PDE in terms of the free surface parameter, η, DFSBC results in a PDE in terms of the velocity potential or the horizonal velocity component. Alternative forms of the Boussinesq equations for different reference velocities can be given for example the velocity at the mean water plane, or a depth averaged velocity can be used. In some models, total instantaneous volume flux is used.

Since the nonlinear term appearing in the Boussinesq equations has a small coefficient, they are generally termed as weakly nonlinear equations. Also, Boussinesq equations are expressed with the order of accuracy selected during derivation process and this implies that they are not exact.

On the other hand, Boussinesq equations can be expressed in one variable if the waves are assumed to travel in one direction. This way it is possible to eliminating either one of the parameters.

Expression of fourth order Boussinesq equations in the free surface parameter,η, is first found in Boussinesq (1872). Korteweg and deVries (1895) uses the assumption that waves are propagating only in one direction to derive the so-called Korteweg-deVries (KdV) equation which is a third order Boussines equation in one variable.

Benjamin et al. (1972) shows that there are not unique forms of the KdV equation and the Boussinesq equation so that it is possible to obtain alternative forms by interchanging the order of derivations with respect to different parameters. Mei (1983) proposes alternative forms of the Boussinesq equation.

Over a one dimensional domain of constant depth, imposing the condition waves propagate only in one direction makes it possible to solve KdV equations analytically leading to cnoidal wave solution that are of constant form. Cnoidal waves are valid in

Table 2.5. Boussinesq Wave Model Properties

Wave Theory	Boussinesq Wave Model
Characteristic Parameters	$H/d << 1$, $U_R \approx 1$
Range of Validity	Shallow Water ($d/L < 0.05$)(There are extension efforts)
Assumptions	Irrotational, Nonhydrostatic, Perfect fluid,
	Translatory, Exact (1st Order Theory),
	Non-exact (higher orders),
	Higher order models are numerical,
	Up to 2D horizontal domain,
	Varying impermeable bottom, Negligible surface tension

Figure 2.1. Validity of water wave theories by Le Méhauté (1976)

the shallow water region giving results better than linear shallow water wave model. Therefore, it is better to use cnoidal wave model in shallow water compared to linear and Stokes wave models. Cnoidal wave profile is expressed in terms of a Jacobian elliptic integral, numerical algorithm of which is given in Press et al. (1986).

In the Figure 2.1, an updated version of Le Méhauté's (1976) study comparing water wave models is given. As it can be seen, Stokes waves are better in deep water while cnoidal works well in shallow water, linear wave theory has better performance at intermediate water and stream function waves at different orders work well at any depths.

Also, for the case of inifinitely long waves cnoidal waves reduce to the solitary waves which are in the form of single crest and the free surface, η, is greater than zero everywhere. Applications of solitary wave model can be found in Munk (1949).

Extension of Boussinesq model into two dimensional horizontal domain with vary-

ing depth is derived in Peregrine (1967) where equations are given in terms of the depth averaged velocity and linear dispersion characteristic is diplayed clearly. A detailed review of the topic is given in Madsen and Schäffer (1998).

In the literature, several efforts to enhance the deep water properties of the Boussinesq wave models can be found. The idea is based on the fact that phase velocity shows dependency on the highest order linear terms in the equations as water depth increases.

On the other hand, Madsen et al. (1991) show a form of the equation with linear dispersion characteristics dependent on a parameter that is optimized with least squares and it shows better linear dispersion characteristics compared to Stokes waves in deep water. This study is taken further in Madsen and Schäffer (1998) where a linear differential operator termed as *linear enhancement operator* is proposed to ehance deep water behavior of the Boussinesq wave model.

On the other hand, Nwogu (1993) shows similar enhancement to Madsen et al. (1991) by expressing the Boussinesq equations at an arbirtary depth. Therefore, this study sets a relationship between the arbitrary depth and the optimum enhancement parameter found by Madsen et al(1991).

Another Boussinesq equations are made made fully nonlinear within the literature of extension efforts of the model. Serre (1953) derived fully nonlinear equations keeping nonlinear terms omitted in the classical derivations. Wei et al. (1995) examines the accuracy of the fully nonlinear Boussinesq models.

There are also efforts to extend the accuracy of Boussinesq models by increasing the order of equations. Gobbi and Kirby (1999) and Gobbi et al.(2000) used the average of two reference velocities and introduced fifth order derivatives into the equations.

Besides, Yoon and Liu (1989) and Chen et al. (1998) develops a Boussinesq model that took the interaction of waves with currents into account. Agnon et al. (1999) and

Madsen et al. (2002, 2003), express boundary conditions on the bottom and the free surface at the still water level in terms of horizontal and vertical velocity components along with a truncated expansion solution for the Laplace equation and succeeded in developing higher order Boussinesq models.

Furthermore as a successful numerical solution methodology Wei and Kirby (1995)'s Adams-Bashforth-Moulton (ABM) integration method and frequency domain method of Kaihatu (2003) are important to revise.

Also, for the purpose of including wave breaking,a viscosity or a diffusion term is added to the Boussinesq equations in the following studies, Zelt (1991), Karambas and Koutitas, Wei et al. (1995), Kennedy et al. (2000).

Similarly, Brocchini et al. (1992) and Schäffer et al. (1993) introduce roller method and Veramony and Svendsen (1998, 2000) introduce viscous dissipation by splitting the equation of motion into a potential and a rotational part to implement wave breaking.

Since the developments in the Boussinesq modeling literature is exhaustive following extensive reviews can be given for futher reference, i.e. Kirby (1997, 2003), Brocchini and Landrini (2013).

2.3.3. Nonlinear Shallow Water Wave Models

In nonlinear Shallow Water Equations (NSWE) characteristics coefficient of the nonlinear terms is an order 1 ($O(1)$) quantity. And, this makes them strongly nonlinear. In these models, velocity is assumed to be constant over the depth so that expressions in terms of the depth averaged velocity are present in the literature.

There exists analytical and numerical solutions to nonlinear equations in the studies like Thacker (1981), Synolakis (1987), Liu et al. (1995) and Titov and Synolakis (1997), Kanoğlu (2004). Also, there are several numerical models focused on tsunami

wave propagation and run up in the literature.

2.4. Linear Uneven Bathymetry Model; Mild-Slope Equation

Within the literature of small amplitude waves, due to the need for including the bottom variation into the models, mild-slope equation was developed by Eckart(1952) and later by Berkhoff (1972, 1976). It was an improvement to its predecessor ray tracing method and based on the assumption of mildly varying bathymetry. This assumption lead to the conclusion that that a monochromatic wave propagates with its primary mode only and the evanescent modes are negligible. Further studies have been made by Kirby and Dalrymple (1983), Tsay and Liu (1982) to overcome the difficulty of specifying shoreline boundary conditions and a parabolic approximation introduced into the mild-slope equation.

2.5. Other Fully Nonlinear Potential Theory(FNPT) Models

Apart from the fully nonlinear Boussinesq models reviewed before, there are Laplace equation based full 3D or 2D models present in the literature. These models throughout the domain of interest make use of the potential theory and use Laplace Equation as the governing equation and construct a system imposing the boundary conditions of the flow. Although Laplace Equation is a linear PDE, nonlinearity is due to the free surface boundary conditions. Also, time dependency is introduced through free surface boundary conditions since the Laplace Equations is a steady state PDE.

Validity of these models covers the entire range of water depths. However, Laplace equation based models assume that the fluid is ideal therefore there is no internal friction. Secondly, flow field is irrotational. This assumption is violated when irregularities on the boundaries surrounding the fluid find time to cause substantial energy dissipation or when waves approach to the breaking point where the fluid becomes rotational. These numerical models are more accurate than the models with limited range of applicability, but requires much more computational power.

Romate (1989) and Broeze (1993) uses the boundary element method (BEM), Kennedy and Fenton (1996, 1997) uses polynomials, Li and Fleming (1997) uses a finite difference multgrid model in their 3D Laplace wave models. A more detailed review on these models can be found in Ma (2010).

2.6. Navier Stokes Models

Another class of fully nonlinear wave models is the NS models based on the NS equations which are composed of momentum equations and the continuity equation. NS Equations can be of several forms and when necessary they are coupled with other physics like thermodynamics or magnetohydrodynamics. However, incompressible, Newtonian, isotropic fluids momentum equations and the continuity are satisfactory and detailed derivation can be found in Eringen (1980) and Schlichting (1979).

Analytical solutions present for the NS Equations are limited since they are obtained after some simplifications and assumptions. Therefore they are limited to a small set of flows. In the case of water wave propagation, when a detailed understanding is required on the processes due to waves, analytical models are unsatisfactory and numerical models are inevitable.

Compared to the models reviewed until this point NS models are more general and free of some of the limitations those models have. Moreover, they are valid for entire depths of water. One other superior aspect of the NS Equations is that viscosity is present in them and hence no artificial term is needed to account for viscous dissipation generally used to expand the capabilities of inviscid models.

There are also some drawback for NS models. First, they are difficult to implement. For example the pressure appears indirectly (with its gradient) in the equations and there no other independent equations of the pressure to solve it directly. Instead, there is the continuity equation that relates the gradient of the velocity components. Therefore generally an equation for the pressure is derived form the momentum equations and its solution guarantees the satisfaction of the continuity. And, in projection

methods, the resulting equation obtained from the addition of the derivatives of the momentum equations with respect to directions they are defined along is an elliptic type Poisson equation.

On the other hand, NS equations can be simplified with the definition of a stream function on the plane where the resulting governing equation is a Poisson equation. These models are called the stream-function vorticity models because the equation displays the connection between the stream function and the vorticity. However, these models are restricted to a plane and since extension of them to 3D brings some other difficulties, they are not popular for water wave propagation problems.

On the other hand, NS Equations can be modeled directly with special techniques. These techniques can be listed as explicit/implicit time marcing methods, artificial compressibility methods and fractional step methods. Details of these methods can be found in the texts Ferziger and Perić (2002), Cebeci et al. (2005), Versteeg and Malalasekera (2007).

There are two options for the time marching methods. Variables are discretized in time either explicitly or implicitly. When an explicit expression is used, a divergence free velocity field is needed for the new time step. Therefore, a pressure equation is derived using the continuity equation and its solution guarantees the velocity field at the new time step to be divergence free.

Alternatively, implicit discretization leads to large systems of equations and due to nonlinear nature of the problem, the coefficient matrix also depend on the unknowns of the new time step and direct solution is impossible. Therefore, iterative solution methods are employed and depending on the problem size, these methods can be very costly in terms of computer resources and implicit methods are developed to reduce the costs of computation. These methods can be listed as Semi-Implicit Method for Pressure-Linked Equations (SIMPLE) of Patankar and Spalding (1972), SIMPLER (SIMPLE Revised) of Patankar (1980), SIMPLEC (SIMPLE Consistent) of Van Doormal and Raithby (1984), Pressure Implicit with Splitting of Operators (PISO) of Issa

(1986).

Turbulent characteristics of a flow is an important issue in models. Turbulent behavior in wave models is observed due to anomalities at the boundaries and wave breaking. First of the three mostly used methods is the Reynold Averaged Navier Stokes (RANS) model where RANS Equations are derived by splitting the mean flow parameters and the turbulent fluctuations and then they are coupled with a transport model. Widely used transport model is the $k-\epsilon$ model proposed by Launder and Spalding (1974). Later in Speziale (1987) a nonlinear $k-\epsilon$ model developed. Wilcox's (1988, 1993a, b, 1994) $k-\omega$ model and Menter's (1992a, b, 1994,1997) shear stress transport (SST) $k-\omega$ model are common alternatives to the $k-\epsilon$ model. Since the literature of the topic is very exhaustive more details can be found in Ferziger and Perić (2002), Versteeg and Malalasekera (2007), Cebeci (2004).

Second method used in turbulence models is the Large Eddy Simulation (LES) method in which large eddies are computed by space filtering out small scale eddies and effect of small eddies are included with a subgrid scale model. These models demands more computer resources than the RANS models. Finally, third approach to model the turbulent behavior is employed in Direct Numerical Simulation (DNS) models. In DNS models, spatial grids are sufficiently fine and time steps are sufficiently small to capture every necessary length scales and fluctuations. However, the DNS models require the most computer resources compared to alternatives.

One other inherent difficulty in NS equations based wave propagation models is due to the free surface deforming in time. There are studies using a σ-coordinate transformation that maps the vertical coordinate into $\sigma = 0$ on the bottom and $\sigma = 1$ on the surface. For example, Li and Fleming (2001), Lin and Li (2002), Yuan and Wu (2004), Li (2008), Ma et al. (2015) used σ transformation to define the free surface boundary conditions exactly. Major drawback of the σ coordinate transformation is because of the multiple-valuedness of the free surface which occurs when the waves start to overturn.

On the other hand, several alternative methods that are tracking the free surface with a specific approach without using any transformations have been developed. Harlow and Welch (1965) developed the Marker and Cell (MAC) method in which the free surface is tracked by massless particles. Longuet-Higgins and Cokelet (1976) used Lagrangian descriptions of the free surface boundary conditions. Hirt et al. (1975) developed Arbitrary Lagrangian-Eulerian (ALE) method applicable to greater deformations handled by purely Lagrangian approach. Alfrink and van Rijn (1983) used an integral method to compute free surface displacements. Hirt and Nichols (1987) proposed Volume of Fluid (VOF) method in which fractional values are used to describe the computational cells containing the free surface. Osher and Sethian (1988) constructed a level-set equation to track the position of the free surface in their Level Set Method (LSM). Monaghan (1992) developed Smooth Partial Hydrodynamics (SPH) method where free surface is defined by particles whose properties are smoothed by a function. In their studies Kennedy and Fenton (1996, 1997) applied the semi-Lagrangian approach in which they used the Eulerian description of the dynamic free surface boundary conditon (DFSBC) and Lagrangian description of the free surface velocity potential.

2.7. Radial Basis Function Collation Methods

For a set of collocation centers defined at locations $\mathbf{x}_i$ on a problem domain Ω where i is from 1 to N, it is possible to express a field variable using radial basis functions (RBFs) that are functions of the Euclidean distances between these centers. Namely,

$$y(\mathbf{x}) = \sum_{j=1}^{N} \alpha_j \varphi(|\mathbf{x} - \mathbf{x}_j|, \epsilon) \tag{2.2}$$

where y is a field variable, $|\mathbf{x} - \mathbf{x}_j|$ is the disatance between center located at any arbitrary location $\mathbf{x}$ on the domain and $\mathbf{x}_j$ is the location of a center at j. Also, ϵ is a shape parameter present in some RBFs.

The standard RBFs can be classified as globally supported compactly supported. In Table 2.6 some commonly used globally supported RBFs and in Table 2.7 compactly supported RBFs due to Wendland (1995) are given. Apart from these traditional RBFs, there are problem dependent RBFs and Kernel RBFs.

In Hardy (1971), the multiquadric radial basis functions (MQRBF) method is used to interpolate the geophysical surfaces. Similarly, based on the bending theory of a thin plate, thin plate spline (TPS) is used in Duchon (1975). In the study Franke (1982) interpolation of scattered data with is compared with different methods and MQRBF is the most accurate methods among the 29 methods used in the comparison. In Kansa (1990a, 1990b) elliptic, parabolic and hyperbolic type PDEs are solved using unsymmetric collocation method. It is shown in Wertz et al. (2006) that there is no need to augment the approximate definition of variables with polynomials according to unsymmetric collocation method of Kansa (1990a, 1990b).

In order to increase the accuracy and improve the stability, in Fedoseyev et al. (2002), extra RBF centers are defined close to the boundary outside the domain. These centers provided space for additional equations to be used in the resulting square linear system. Therefore, the governing PDE is used on the boundary centers along with the boundary conditions.

In Chen (2002) Kansa's unsymmetric collocation method is modified and a symmetric Hermite formulation is proposed. This method does not use and extra collocation centers close to the boundaries and makes use of the advantages of symmetric linear system.

On the other hand, within the context of boundary element method (BEM), Kupradze and Aleksidze (1964) pioneer the development of the method of fundamental solutions (MFS). In MFS the homogeneous type problems are discretized on the boundary and approximate definitions to variables use the RBFs as the fundamental solutions of the governing differential operators. Also, non-homogeneous problems are solved by coupling the MFS by some other methods for the evaluation of the particular

Table 2.6. Some commonly used RBFs with global support

Piecewise Smooth RBFs	$\varphi(r)$
Piecewise Polynomial	$\|r\|^n$, n odd
Thin Plate Spline	$\|r\|^n \ln \|r\|$, n even
Infinitely Smooth RBFs	$\varphi(r, c)$
Multiquadric(MQ)	$\sqrt{r^2 + c^2}$
Inverse Multiquadric	$\frac{1}{\sqrt{r^2+c^2}}$
Gaussian	e^{-cr^2}

Table 2.7. Wendland's positive definite functions with compact support

Dimension	$\varphi(r)$	Smoothness
1	$(1-r)$	C^0
	$(1-r)_+^3(3r+1)$	C^2
	$(1-r)_+^5(8r^2+5r+1)$	C^4
2	$(1-r)_+^2$	C^0
	$(1-r)_+^4(4r+1)$	C^2
	$(1-r)_+^6(35r^2+18r+3)$	C^4
	$(1-r)_+^8(32r^3+25r^2+8r+1)$	C^6

solution according to PDE splitting approach of Chen (2002).

The global collocation methods are using all of the centers defined on a domain and this results in dense system matrices that are sometimes ill-conditioned and computationally expensive to solve. Especially to large scale time dependent problems, global methods are not applicable. Therefore, several efforts have been made to eliminate these problems.

As listed in the Table 2.7, using compactly supported RBFs is a solution to avoid

dense matrices. In Wong et al. (199), the domain is divided into separate zones to reduces the matrix sizes. On the other hand, some local methods like RBF-Finite Differences (RBF-FD) method have been developed for the same purpose. Like the finite difference coefficients obtained from the Taylor series expansion of parameters around a point of interest, a collocation scheme involving neighboring centers are set up to find their weights. And, using these weights a sparse linear system is obtained. Details of the method can be found in studies Fornberg et al. (2013), Flyer et al. (2015), Fornberg and Flyer (2015).

A detailed review of the RBF literature accumulated over the past couple of decades can be found in Chen et al. (2014).

3. MATHEMATICAL MODEL

In this chapter, mathematical definition of the wave propagation problem is introduced along with the assumptions and boundary conditions. Some of the assumptions are fundamental so that their existence restricts the applicability of the problem to a specific set of cases, whereas some are less effective as the applicability of the model can be extended through some additional implementations. Non-fundamental assumptions are selected in a way to meet the purposes of the study.

3.1. Problem Definition

Mathematical model of the problem is based on the following assumptions

- The flow is unsteady.
- Incompressible.
- Viscous.
- Rotational effects caused by the irregularities on the boundaries do not have enough time to alter the flow field within the time scale of the tests, i.e. viscosity is taken constant. However, it is possible to implement the variation of the viscosity throughout the flow field by coupling the model with a $k-\epsilon$ turbulence model.
- Model verification cases are selected so that all of the wave properties and the physical conditions do not change in the transverse direction. Therefore, definitions and formulations are made in 2D. As it will be apparent in the next chapter where the numerical formulation of the problem and its implementation is presented, accounting for the 3D problems requires not more than the additional boundary conditions and more computer resources.
- Bottom boundary is rigid and impermeable.
- Density of the water is constant throughout the domain.

Under these assumptions NSE describing the wave motion can be defined by the

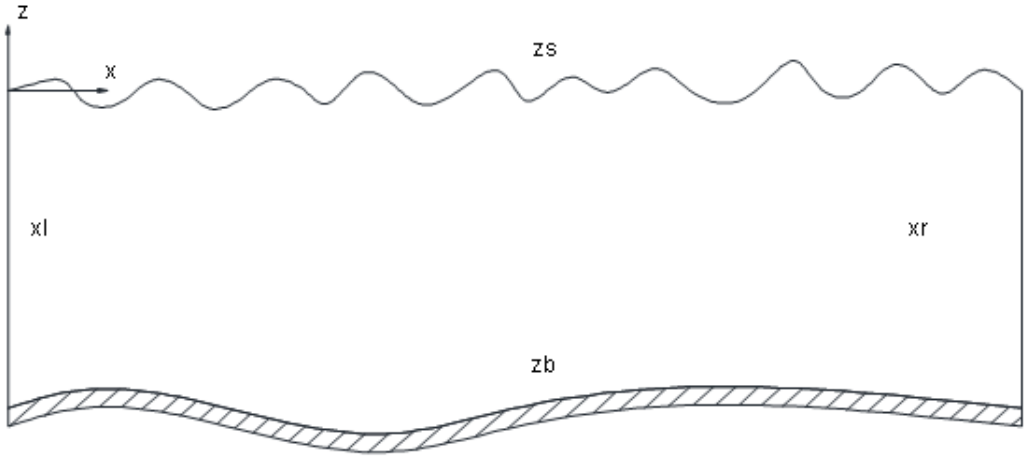

Figure 3.1. Problem definition sketch

following momentum equations and the continuity.

$$\frac{u}{t} + u\frac{u}{x} + w\frac{u}{z} = -\frac{p}{x} - g\frac{\eta}{x} + \nu\nabla^2 u \tag{3.1}$$

$$\frac{\partial w}{\partial t} + u\frac{\partial w}{\partial x} + w\frac{\partial w}{\partial z} = -\frac{\partial p}{\partial z} + \nu\nabla^2 w \tag{3.2}$$

$$\frac{\partial u}{\partial x} + \frac{\partial w}{\partial x} = 0 \tag{3.3}$$

where $x_L \leq x \leq x_R$, $z_b(x) \leq z \leq \eta(x,t)$ as illustrated in the Figure 3.1. Also, $u = u(x,z,t)$ and $w = w(x,z,t)$ are the velocity components in the horizontal and vertical direction respectively, $p = p(x,z,t)$ is the dynamic pressure per unit density of water, $\eta = \eta(x,t)$ is the free surface, ν is the kinematic viscosity of water, t is time and g is the gravitational acceleration.

Since the density is assumed as constant, it is incorporated in the pressure gradient so that pressure per unit density of water is used in the Equations 3.1 and 3.2.

Also the dynamic and hydrostatic pressure components are separated.

$$p_t = g(\eta - z) + p \tag{3.4}$$

where p is the dynamic part of the wave dynamic pressure, p_t is the total pressure. Hydrostatic part of the wave dynamic pressure is included in the hydrostatic term as shown. Pressure terms in this equation are in per unit density of water. Using this definition, the corresponding pressure gradients can be obtained follows.

$$\frac{\partial p_t}{\partial x} = g\frac{\partial \eta}{\partial x} + \frac{\partial p}{\partial x} \tag{3.5}$$

and

$$\frac{\partial p_t}{\partial z} = -g + \frac{\partial p}{\partial z} \tag{3.6}$$

Eventually, the gravitational effect appearing in the vertical momentum equations disappears while an additional term containing the free

3.2. Initial Condition

Two alternative initial conditions are employed in the model. In one of the conditions, simulations are started in an already formed flow field while cold starting simulations start with a calm water. In the former, it is required that the field parameters are known at the beginning, $t = t_0$, that is,

$$u(x, z, t_0) = u_0 \qquad w(x, z, t_0) = w_0 \qquad \eta(x, t_0) = \eta_0 \tag{3.7}$$

The other field variable, namely the dynamic pressure, is not necessarily known at the beginning due to the implementation of pressure field coupling method that will be explained in detail in the next chapter.

Also, for cold starting simulations the initial values become

$$u(x,z,t_0)=0 \qquad w(x,z,t_0)=0 \qquad \eta(x,t_0)=0 \tag{3.8}$$

3.2.1. Input Boundary Condition

For right going waves, input boundary condition is defined on the left end truncation boundary at a location $x = x_L$ such that $x_L < x_R$ where x_R is the location of the right end truncation boundary. Wave properties are assumed to be known at any time on this boundary.

There are studies present in the literature using the linear wave theory as the input boundary condition. However, in order to account for more general waves and to overcome the difficulty in the application of the linear wave theory where the free surface is assumed on the mean water level, stream function waves found in Chappelear(1961) and Dean(1965) are used. Since the stream function wave parameters are computed numerically, Fourier method solution of Fenton (1988) is employed. In this method, stream function $\psi(x,y)$ in a reference frame moving with the wave is expressed as

$$\psi(x,y) = -\tilde{u}(d+z) + \left(\frac{g}{k^3}\right)^{1/2} \sum_{j=1}^{N} B_j \frac{\sinh jk(d+z)}{\cosh jkd} \cos jkx \tag{3.9}$$

where $\tilde{u}$ is the mean flow velocity, d is local depth at the input boundary, B_j are dimensionless constants k is the wave number, N_s is the order of the stream function. This expression satisfies the bottom boundary condition exactly. Therefore in order to obtain the unknown coefficients, an independent equation set is constructed using the KFSBC and pressure boundary condition on the surface along with some other independent equations relating the wave parameters. And the following field parameters on fixed frame are obtained from the stream function and Fourier series interpolation.

$$\eta(x_L,t) = \sum_{j=1}^{N_s-1} B_j \cos jk(x_L - Ct) + \frac{1}{2} B_{N_s} \cos N_s k(x_L - Ct) \tag{3.10}$$

$$u(x_L, z, t) = C - \bar{u} + \sqrt{\frac{g}{k}} \sum_{j=1}^{N_s} jB_j \frac{\cosh jk(h+z)}{\cosh jkh} \cos kj(x_L - Ct) \tag{3.11}$$

$$w(x_L, z, t) = \sqrt{\frac{g}{k}} \sum_{j=1}^{N_s} jB_j \frac{\sinh jk(h+z)}{\cosh jkh} \sin kj(x_L - Ct) \tag{3.12}$$

$$p(x_L, z, t) = r - g\eta - \frac{1}{2}\left[(u - C)^2 + w^2\right] \tag{3.13}$$

where r is the Bernoulli constant and C is the wave phase speed.

3.2.2. Free Surface Boundary Conditions

On the free surface $z = \eta$, it is assumed that the surface tension is negligible and there no other external forces like the wind. Therefore, corresponding kinematic free surface boundary condition is as follows.

$$\frac{\partial \eta}{\partial t} + u_s \frac{\partial \eta}{\partial x} = w_s \tag{3.14}$$

where u_s and w_s are the components of the velocity field on the surface, namely,

$$u_s = u(x, z = \eta(x,t), t) \qquad w_s = w(x, z = \eta(x,t), t) \tag{3.15}$$

Therefore a Semi-Lagrangian description of the time rate of change of velocity components on the free surface becomes

$$\frac{\partial u_s}{\partial t} = \frac{\partial u}{\partial t}\Big|_{z=\eta} + \frac{\partial u}{\partial z}\frac{\partial \eta}{\partial t} \tag{3.16}$$

Figure 3.2. Bottom boundary sketch.

$$\frac{\partial w_s}{\partial t} = \frac{\partial w}{\partial t}\Big|_{z=\eta} + \frac{\partial w}{\partial z}\frac{\partial \eta}{\partial t} \tag{3.17}$$

so that the centers are allowed to move with the free surface at fixed horizontal locations. One other alternative approach to this kind of surface tracking is the fully Lagrangian approach where collocation centers on the surface are free to move in any direction. This requires the full Lagrangian descriptions of the free surface boundary conditions. In this study only the Semi-Lagrangian approach is implemented in the model.

Also, when there is no ambient pressure, the gauge pressure on the free surface is expressed as

$$p(x, z = \eta, t) = 0 \tag{3.18}$$

3.3. Bottom Boundary Condition

For a rigid and impermeable boundary, no flux boundary condition is valid, that is

$$\mathbf{v} \cdot \mathbf{n} = 0 \tag{3.19}$$

where $\mathbf{v}$ is the velocity vector and $\mathbf{n}$ is an arbitrary length bottom boundary normal vector. For a bottom defined as $z = z_b(x)$, normal vector can be derived either geometrically as illustrated in Figure 3.2 or using the gradient vector.

From the Figure 3.2, a bottom boundary normal can be given in the form

$$\mathbf{n} = \frac{\partial z_b}{\partial x}\mathbf{i} + \mathbf{j} \tag{3.20}$$

as the slope $\tan\beta$ of the boundary tangent is equal to $\partial z_b/\partial x$. Or, alternatively the gradient operator can be used to define the bottom boundary normal.

$$\nabla z_b = \frac{\partial z_b}{\partial x}\mathbf{i} + \mathbf{j} \tag{3.21}$$

Once the bottom boundary vector is defined, it is possible to write the impermeable and rigid bottom boundary condition explicitly.

$$u\frac{\partial z_b}{\partial x} + w = 0 \tag{3.22}$$

In the numerical formulation of the problem, this boundary condition is used to project the momentum equations without the convective terms to derive a bottom boundary condition of the pressure. Since the pressure field obtained using this condition is used to correct the velocity field accordingly, using the Equation 3.22 explicitly on the velocity components becomes unnecessary.

3.4. Radiation Boundary Condition

On the radiation boundary which is at a distance integral multiple of the wavelength, it is assumed that wave properties repeat themselves for periodic simulations. Namely, at $x = x_R = x_L + mL$ where x_L and x_R are the locations of the input and radiation boundary respectively, m is an integer, L is the wavelength, wave parameters can be expressed as

$$u(x_R, z, t) = u(x_L, z, t) \qquad w(x_R, z, t) = w(x_L, z, t) \qquad \eta(x_R, z, t) = \eta(x_L, t) \tag{3.23}$$

and since the flow properties of the input boundary is expected to be repeated on the radiation boundary, flow field must be formed at the beginning. Therefore, periodic boundary condition cannot be used in cold starting simulations.

On the other hand, for the cases where the wave properties are not known at the outgoing boundary, Sommerfeld (1949) radiation boundary condition(RBC) can be used alone or coupled with the sponge layer of Israeli and Orszag (1981).

The Sommerfeld RBC poses the advection of a field variable φ in the form

$$\frac{\partial \varphi}{\partial t} + c\frac{\partial \varphi}{\partial x} = 0 \tag{3.24}$$

where c is a constant. If the phase speed of the waves arriving at the radiation boundary is known, then it can be used for c. However, in more complex cases, wave phase speed cannot be determined. So, the following approximate estimate is used

$$C_n = -\frac{\varphi_i^{n+1} - \varphi_i^n}{\varphi_i^{n+1} - \varphi_{i-1}^{n+1}} \tag{3.25}$$

which is a forward implicit method due to Miller and Thorpe (1981). In this numerical expression, superscript denotes the time step and $n+1$ refers to the next time step of integration performed at time step n and subscript denotes the discrete locations of field variables where i is the location on the radiation boundary and $i-1$ is the closest location next to the radiation boundary. The relationship between the c in Sommerfeld RBC and C_n is as follows.

$$C_n = c\frac{\Delta t}{\Delta x} \tag{3.26}$$

where Δt is the time step and Δx is the distance between the between the radiation boundary and the discrete location closest to the radiation boundary.

The form proposed by Miller and Thorpe (1981) is simply the ratio of the first order discretizations of the derivatives appearing in the Sommerfeld RBC. Namely, the factor c is left alone

$$c = -\frac{\partial \varphi}{\partial t} / \frac{\partial \varphi}{\partial x} \tag{3.27}$$

Figure 3.3. Variation of sponge coefficient for c_s with respect to x/L_s which is the normalized distance of x from starting point of the sponge layer.

where the time rate of change is discretized using the Euler's scheme at location i on the radiation boundary from time t_n to t_{n+1}

$$\frac{\partial \varphi}{\partial t} \approx \frac{\varphi_i^{n+1} - \varphi_i^n}{\Delta t} \tag{3.28}$$

and the spatial derivative is discretized according to the backward finite differences scheme at time t_{n+1}

$$\frac{\partial \varphi}{\partial x} \approx \frac{\varphi_i^{n+1} - \varphi_{i-1}^{n+1}}{\Delta x} \tag{3.29}$$

On the other hand, sponge layer is introduced into the momentum equations with an artificial term according to Israeli and Orszag (1981).

$$\frac{\partial u}{\partial t} + u\frac{\partial u}{\partial x} + w\frac{\partial u}{\partial z} = -\frac{\partial p}{\partial x} - g\frac{\partial \eta}{\partial x} + \nu\nabla^2 u - c_s(x)u \tag{3.30}$$

$$\frac{\partial w}{\partial t} + u\frac{\partial w}{\partial x} + w\frac{\partial w}{\partial z} = -\frac{\partial p}{\partial z} + \nu\nabla^2 w - c_s(x)w \tag{3.31}$$

where c_s is the damping coefficient of the sponge layer and on $0 \leq x \leq L_s$ it is given as

$$c_x(x) = \frac{exp(x/L_s) - 1}{exp(1) - 1} \tag{3.32}$$

where L_s is the length of the sponge layer. c_S attains its maximum value 1 right at the radiation boundary and its minimum at the starting location of the sponge layer. Variation of c_s is illustrated in Figure 3.3.

In a more detailed definition of sponge layer, Wei and Kirby (1995) use an additional term like an artificial viscous damping term and add extra coefficients to adjust

the slope of the coefficients. So, the damping terms $w_1(x)$ and $w_2(x)$ added to the momentum equations on $x_s \leq x \leq x_f$

$$\frac{\partial u}{\partial t} + u\frac{\partial}{u}\partial x + w\frac{\partial u}{\partial z} = -\frac{\partial p}{\partial x} - g\frac{\partial \eta}{\partial x} + \nu\nabla^2 u - w_1(x)u - w_2(x)\nabla^2 u \tag{3.33}$$

$$\frac{\partial w}{\partial t} + u\frac{\partial w}{\partial x} + w\frac{\partial w}{\partial z} = -\frac{\partial p}{\partial z} + \nu\nabla^2 w - w_1(x)w - w_2(x)\nabla^2 w \tag{3.34}$$

are expressed as

$$w_1(x) = \alpha_1 \omega f(x) \tag{3.35}$$

$$w_2(x) = \alpha_2 \omega f(x) \tag{3.36}$$

where

$$f(x) = \frac{exp\left(\frac{x-x_s}{L_s}\right)^r - 1}{exp(1) - 1} \tag{3.37}$$

with ω being the frequency of the wave, α_1, α_2, r being the constants to be determined by trial and error. With this version of sponge layer coefficients, it is possible adjust the slopes of the damping coefficient c_s shown in Figure 3.3. It is expected that the better these slopes match the natural variations of the parameters at the interface between the real problem domain and the sponge layer, the less reflection occurs from this interface.

4. NUMERICAL METHODOLOGY

In the first part of this chapter numerical discretization of the problem in time is presented along with the methodology that provides the means for the solution of the pressure field. Beause there are no other independent equation for the pressure and the remaining equation other than the momentum equations is the continuity which is an equation of the velocity field only, an equation for the pressure is derived. In the the second part RBF approximations of the problem is introduced along with the selected numerical method that determines how the equation sets are defined both for the computation of the velocity components and the pressure field. In the third part of this chapter, time marching methods implemented in the model are presented. And in the final part software design methodology of the model is discussed and a flow chart of the model is given.

4.1. Explicit Discretization In Time and The Pressure Equation

According to the projection method of Chorin (1968) and Temam (1969), initially provisional values for the velocity field are obtained from the momentum equations without the pressure terms. Namely,

$$\frac{u^* - u^n}{\Delta t} + u^n \frac{\partial u^n}{\partial x} + w^n \frac{\partial u^n}{\partial z} = \nu \nabla^2 u^n \tag{4.1}$$

$$\frac{w^* - w^n}{\Delta t} + u^n \frac{\partial w^n}{\partial x} + w^n \frac{\partial w^n}{\partial z} = \nu \nabla^2 w^n \tag{4.2}$$

where u^* and w^* are the provisional velocity components. Superscript n denotes the time step of the previous step, therefore this formulation corresponds to the initial provision of the velocity field for the new time step $n+1$. In the second step of the pressure correction method, the velocities are corrected to obtain the velocity field at

the new time step $n+1$ as in the following.

$$\frac{u^{n+1}-u^*}{\Delta t} = -\left(\frac{\partial p_d^{n+1}}{\partial x} + g\frac{\partial \eta^n}{\partial x}\right) \tag{4.3}$$

$$\frac{w^{n+1}-w^*}{\Delta t} = -\frac{\partial p_d^{n+1}}{\partial z} \tag{4.4}$$

This correction step requires the computation of the pressure field at the new time step. Computing the derivative of the Equation 4.1 with respect to x and Equation 4.2 with respect to z before summing them together while using continuity whenever necessary following Poisson type elliptic differential equation the pressure field at the new time step is obtained.

$$\nabla^2 p_d^{n+1} = \frac{1}{\Delta t}\left(\frac{\partial u^*}{\partial x} + \frac{\partial w^*}{\partial z}\right) - g\frac{\partial^2 \eta}{\partial x^2} \tag{4.5}$$

This elliptic differential equation is subject to

$$p = 0 \tag{4.6}$$

on $z = \eta$. The bottom boundary condition can be obtained by projecting the Equations 4.3 and 4.4 using the impermeable bottom boundary condition $\mathbf{v}^{n+1}\cdot\mathbf{n} = 0$. Therefore, the bottom boundary condition on $z = z(x)$ becomes

$$-\frac{\partial p^{n+1}}{\partial x} + \frac{\partial p^{n+1}}{\partial z} = \left(-g\frac{\partial \eta^n}{\partial x} + \frac{u^*}{\Delta t}\right)\left(-\frac{\partial z_b}{\partial x}\right) + \frac{w^*}{\Delta t} \tag{4.7}$$

In a similar manner, the pressure boundary condition on the radiation boundary

is as follows.

$$\frac{\partial p}{\partial x} = -g\frac{\partial \eta^n}{\partial x} + \frac{u^*}{\Delta t} \tag{4.8}$$

On the input boundary, dynamic pressures per unity density of water are obtained from the input wave given in Equation 3.13.

Explicit time discretization method in the Equations 4.1 and 4.2 is a first order numerical method called the Euler method. In order to minimize the numerical errors that may accumulate in time, this method is replaced by higher order methods. The main objective of using Euler method here is to present the derivation of the projection method. However, computation of the dynamic pressure field and the correction of the velocity field are performed according to the derivations given above.

4.2. Explicit Integration Methods

Two different explicit self starting methods and six different explicit predictor-corrector type multistep integration methods are implemented in the model. Since the multistep methods require information earlier than the results of the most recent integration step, the initiation of the field variables must be performed up to the required number of steps by a self starting method. Therefore, fourth order Runge-Kutta method is implemented for the initiation of the variables at the beginning. Once, there are enough steps to employ methods of higher accuracy, time marching of field variables is performed with higher order multistep methods.

Also, being a predictor-corrector type method where derivatives are computed twice per time step, second order MacCormack method is implemented for the collocation centers that might be entering into the solutions at a later time during the computations depending on the evolution of the free surface. Especially for steep waves, it will be apparent in the following sections that more accurate computation of the vertical momentum equations require collocation centers close to the free surface

above the trough level. This implies that some centers are needed to be enabled or disabled depending on the location of the free surface in time. As a good initiator it is difficult to implement the fourth order Runge Kutta method for the centers enabled at a time step other than the first four steps since it evaluates four times per time step while the other already enabled centers are being integrated with higher order methods evaluating twice per time step. Therefore, MacCormack method evaluating the derivatives twice in a time step keeps pace with the higher order predictor-corrector methods compared to the fourth order Runge Kutta method and initiates the variables at the recently enabled centers up to the required number of time steps by higher order multistep methods.

More detailed information about the methods presented below can be found in Burden and Faires (2001).

4.2.1. MacCormack Method

From time step n to $n+1$, a variable at the new time step y^{n+1} can be obtained as follows.

$$y^* = y^n + \Delta t f(t^n, y^n) \tag{4.9}$$

$$y^{n+1} = \frac{1}{2}\left(y^n + y^*\right) + \frac{\Delta t}{2} f(t^{n+1}, y^*) \tag{4.10}$$

where y^* is the predicted value of the variable, function f is the time rate of change of y and Δt is the time step.

4.2.2. Fourth Order Runge Kutta Method

Value of a variable y at a new time step $n+1$ is computed through

$$\begin{aligned} k_1 &= f(t^n, y^n) \\ k_2 &= f(t^{n+1/2}, y^n + 0.5k_1) \\ k_3 &= f(t^{n+1/2}, y^n + 0.5k_2) \\ k_4 &= f(t^{n+1}, y^n + k_3) \\ y^{n+1} &= y^n + \frac{\Delta t}{6}\left(k_1 + 2k_2 + 2k_3 + k_4\right) \end{aligned} \tag{4.11}$$

where k_1 to k_4 are the intermediate values computed at the beginning, middle and end of the time step. Here, $n + 1/2$ refers to the mid step, namely $t = t^n + 0.5\Delta t$.

4.2.3. Predictor Corrector Methods

?? The predictor corrector methods are explicit multistep methods where the unknown variables are predicted initially with a predictor type integrator and using the predicted values for the new time step, a second evaluation is performed to correct the results. Therefore, these methods cost twice evaluations per time step. Since the unknown values corresponding to time steps earlier than the last computed time step are used, these methods are called multistep methods. In fact, the predictor step is purely explicit in time, whereas the corrector step is implicit in nature. However, the values of the new time step is obtained by the explicit predictor and used in the implicit corrector. Hence, the predictor-corrector methods are explicit methods. The predictor methods are called Adams-Bashforth predictor methods and the corrector methods are called Adams-Moulton corrector methods.

For a variable y being computed from time t^n to t^{n+1} Adams-Bashforth predictor methods of order two to six are as follows.

$$y^* = y^n + \frac{\Delta t}{2}\left[3f(t^n, y^n) - f(t^n, y^{n-1})\right] \tag{4.12}$$

$$y^* = y^n + \frac{\Delta t}{12}\left[23f(t^n, y^n) - 16f(t^n, y^{n-1}) + 5f(t^n, y^{n-2})\right] \tag{4.13}$$

$$y^* = y^n + \frac{\Delta t}{24}\left[55f(t^n, y^n) - 59f(t^n, y^{n-1}) + 37f(t^n, y^{n-2}) - 9f(t^n, y^{n-3})\right] \tag{4.14}$$

$$\begin{aligned} y^* = y^n + \frac{\Delta t}{720}\big[&1901f(t^n, y^n) - 2774f(t^n, y^{n-1}) + 2616f(t^n, y^{n-2}) \\ &- 1274f(t^n, y^{n-3}) + 251f(t^n, y^{n-4})\big] \end{aligned} \tag{4.15}$$

$$\begin{aligned} y^* = y^n + \frac{\Delta t}{1440}\big[&4277f(t^n, y^n) - 7923f(t^n, y^{n-1}) + 9982f(t^n, y^{n-2}) \\ &- 7298f(t^n, y^{n-3}) + 2877f(t^n, y^{n-4}) - 475f(t^n, y^{n-5})\big] \end{aligned} \tag{4.16}$$

On the other hand, for a variable y being computed from time t^n to t^{n+1} Adams-Moulton corrector methods of order two to six are as follows.

$$y^{n+1} = y^n + \frac{\Delta t}{12}\left[5f(t^{n+1}, y^*) + 8f(t^{n+1}, y^n) - f(t^{n+1}, y^{n-1})\right] \tag{4.17}$$

$$y^{n+1} = y^n + \frac{\Delta t}{12}\left[5f(t^{n+1}, y^*) + 8f(t^{n+1}, y^n) - f(t^{n+1}, y^{n-1})\right] \tag{4.18}$$

$$y^{n+1} = y^n + \frac{\Delta t}{24}\left[9f(t^{n+1}, y^*) - 19f(t^{n+1}, y^n) - 5f(t^{n+1}, y^{n-1}) + f(t^{n+1}, y^{n-2})\right] \tag{4.19}$$

$$\begin{aligned} y^{n+1} = y^n + \frac{\Delta t}{720}\big[&251f(t^{n+1}, y^*) + 646f(t^{n+1}, y^n) - 264f(t^{n+1}, y^{n-1}) \\ &+ 106f(t^{n+1}, y^{n-2}) - 19f(t^{n+1}, y^{n-3})\big] \end{aligned} \tag{4.20}$$

$$y^{n+1} = y^n + \frac{\Delta t}{1440}\big[475f(t^{n+1}, y^*) + 1427f(t^{n+1}, y^n) - 798f(t^{n+1}, y^{n-1}) + 482f(t^{n+1}, y^{n-2}) - 173f(t^{n+1}, y^{n-3}) + 27f(t^{n+1}, y^{n-4})\big] \tag{4.21}$$

In the implementation of the model each of the predictor method method is coupled with the corrector of the same order and Adams-Bashforth-Moulton Predictor Corrector Method of Order 2,3,4,5 are implemented. These methods are denoted by ABM2, ABM3, ABM4, ABM5 respectively. Also, it is possible to iterate corrector step more than once to enhance the accuracy of the results but it is computed once in the model since the time step was chosen small enough.

4.3. Radial Basis Function Collocation Method

Until now, the continuous mathematical description of the wave propagation problem is given and discretization of the field variables in time is presented. In this section, approximate definitions of the variables at collocation locations and the resulting discrete system of equations obtained from the continuous definitions are presented.

For a set of N centers located throughout the domain, approximate definition of velocity components at the i-th center at time t can expressed as

$$\begin{aligned} u(\mathbf{x}_i, t) &= \sum_{j=1}^{N} \alpha_j^u \varphi(|\mathbf{x}_i - \mathbf{x}_j|, \epsilon) \\ w(\mathbf{x}_i, t) &= \sum_{j=1}^{N} \alpha_j^w \varphi(|\mathbf{x}_i - \mathbf{x}_j|, \epsilon) \end{aligned} \tag{4.22}$$

where $\mathbf{x}_i$ is the location of the i-th center such that $\mathbf{x}_i = x_i\mathbf{i} + z_i\mathbf{j}$ in 2D. Also, radial basis function φ is a function of the distance between center i and j, and ϵ is the shape parameter that controls flatness of the RBFs. As apparent in the equations, this definition makes the numerical method to be termed as global as all of the centers defined throughout the domain are considered in the computation of a variable at an

arbitrary center.

Although, some RBFs do not contain the shape parameter, it is not defined as optional in this definition because all of the RBFs implemented in the model contains this shape parameter. The RBFs implemented in the model are listed below.

$$\varphi(r_{ij},\epsilon) = \sqrt{r_{ij}^2+\epsilon^2} \qquad \text{(Multiquadric RBF, MQRBF)} \tag{4.23}$$

$$\varphi(r_{ij},\epsilon) = 1/\sqrt{r_{ij}^2+\epsilon^2} \qquad \text{(Inverse Multiquadric RBF, IMQRBF)} \tag{4.24}$$

$$\varphi(r_{ij},\epsilon) = 1/\left(r_{ij}^2+\epsilon^2\right) \qquad \text{(Inverse Quadric RBF, IQRBF)} \tag{4.25}$$

$$\varphi(r_{ij},\epsilon) = \exp(\epsilon^2 r_{ij}^2) \qquad \text{(Gaussian RBF,GARBF)} \tag{4.26}$$

where r_{ij} is the distance between the centers i and j.

The spatial derivatives for the velocity components at collocation center i are obtained through,

$$\begin{aligned}
&\frac{\partial u_i}{\partial x} = \sum_{j=1}^{N} \frac{\partial \varphi_{ij}}{\partial x}\alpha_j^u \qquad \frac{\partial u_i}{\partial z} = \sum_{j=1}^{N} \frac{\partial \varphi_{ij}}{\partial z}\alpha_j^u \qquad \nabla^2 u_i = \sum_{j=1}^{N} \nabla^2\varphi_{ij}\alpha_j^u \\
&\frac{\partial w_i}{\partial x} = \sum_{j=1}^{N} \frac{\partial \varphi_{ij}}{\partial x}\alpha_j^w \qquad \frac{\partial w_i}{\partial z} = \sum_{j=1}^{N} \frac{\partial \varphi_{ij}}{\partial z}\alpha_j^w \qquad \nabla^2 w_i = \sum_{j=1}^{N} \nabla^2\varphi_{ij}\alpha_j^w
\end{aligned} \tag{4.27}$$

where the coefficients are obtained from the Equation 4.22 given that the velocity components are known at the collocation center locations.

On the other hand, approximate expression of the dynamic pressure field is similar to the velocity field but the coefficients are obtained solving the boundary value problem given in Equation 4.5 along with the corresponding boundary conditions. For that purpose Kansa's unsymmetric collocation method given in Kansa (1990a,1990b) is used. In this method using the approximate definition, a set of equations from the governing differential equation and the boundary conditions are set up to solve for the

Figure 4.1. PDE collocation on the boundary illustration

coefficients. Since the resulting coefficient matrix is unsymmetric as apparent from the definitions of the variables and their spatial derivatives, the method is also termed as unsymmetric.

Furthermore, as discussed before, since the method defined is a global method, the solutions are very sensitive to the errors developing in time due to the boundaries. This is an inherent problem in numerical methods since there are no information beyond the boundaries and most of the time causes instabilities in the models. Compared to local methods, boundary errors are reflected faster in global methods and the need arises for extra treatments.

The PDE collocation on the boundary method helps to the convergence of the global RBF methods, increases stability and accuracy. As illustrated in the Figure 4.1 for each of the centers on the boundary there is a pairing center just outside the domain close to to the boundary center. These extra collocation centers guarantee a square coefficient matrix and makes it possible to define the boundary condition and the governing equation at the same time at each of the collocation centers on the boundary.

Therefore given that there are M centers on the boundary, approximate definition for the dynamic pressure per unit density of water at a collocation center i can be given as,

$$p(\mathbf{x}_i, t) = \sum_{j=1}^{N+M} \alpha_j^p \varphi(|\mathbf{x}_i - \mathbf{x}_j|, \epsilon) \tag{4.28}$$

and its derivatives can be expressed in a similar fashion to the velocity components as given below.

$$\frac{\partial p_i}{\partial x} = \sum_{j=1}^{N} \frac{\partial \varphi_{ij}}{\partial x} \alpha_j^p \qquad \frac{\partial p_i}{\partial z} = \sum_{j=1}^{N} \frac{\partial \varphi_{ij}}{\partial z} \alpha_j^p \qquad \nabla^2 p_i = \sum_{j=1}^{N} \nabla^2 \varphi_{ij} \alpha_j^p \tag{4.29}$$

4.4. Numerical Discretization of the Free Surface

The free surface variable η at center i can be approximately defined as

$$\eta_i(x_i, t) = \sum_{j=1}^{N_s} \alpha_j^{\eta} \varphi(|x_i - x_j|, \epsilon) \tag{4.30}$$

where the centers are located along a line for 2D problems which makes the collocation a 1D collocation where the distance between the centers i and j is simply obtained by $|x_i - x_j|$. Also the N_s collocation centers located along a line are independent from the collocation centers used for the velocity and pressure field.

Similarly, spatial derivatives of the free surface are obtained as follows.

$$\frac{\partial \eta_i}{\partial x} = \sum_{j=1}^{N_s} \alpha_i^{\eta} \frac{\partial \varphi_i}{\partial x} \qquad \frac{\partial^2 \eta_i}{\partial x^2} = \sum_{j=1}^{N_s} \alpha_i^{\eta} \frac{\partial^2 \varphi_i}{\partial x^2} \tag{4.31}$$

4.5. Program Flow and Essential Modules

From a sequential perspective, the following steps are performed from time T_0 to T_f and it is illustrated in a flowchart given in the Figure 4.2.

(i) Collocation centers are set up and coefficient matrices are computed.

(ii) Unknown parameters u^n, w^n and η^n are initialized for $n = 1$.

(iii) At the beginning of the time step $t = T_0 + (n+1)\Delta t$ where T_0 is the start of simulation, Δt is the step size, time rate of change of the variables f_u^n,f_w^n,f_η^n are computed. Time derivatives of the velocity field is computed using the Equations 4.1 and 4.2 where the pressure terms present in the momentum equations are missing, namely f_u^n and f_w^n are the rate of change of provisional values for the velocity field. On the other hand, rate of change of the free surface is computed according to the KFSBC given in the Equation 3.14.

(iv) Predicted values for the unknowns u^{p*}, w^{p*} and eta^p are computed according to

the predictor step of the explicit time integration method. Superscript p is used to denote the predicted values and the velocity components are marked with $*$ since these values are the provisional values.

(v) Time is incremented by a single step Δt.

(vi) Boundary value problem for the pressure given in Equation 4.5 is setup and solved. And, corresponding pressure gradients are computed according to the equations given in 4.29.

(vii) Velocity field is corrected according to the Equations 4.3 and 4.4.

(viii) Rate of change of the variables are computed with the predicted values, f_u^p, f_w^p and f_η^p.

(ix) As the corrector step of the integration method unknowns u^{n+1*}, w^{n+1*}, η^{n+1} for the new time step $n+1$ are computed.

(x) Corresponding pressure field and the gradients are computed.

(xi) Velocity components u^{n+1*}, w^{n+1*} are corrected to get u^{n+1}, w^{n+1}.

(xii) At the end of the time step, geometry is updated using η^{n+1} and the coefficient matrices are updated accordingly.

(xiii) Computations in steps (iii) to (xii) are repeated until the final time T_f is reached.

However, sequential implementation of the model has many drawbacks since it is difficult to extend the features of the model and reusability is out of consideration. Therefore, modular design approach is used to make the model efficient, reusable and extensible. This also allowed the separation of the related tasks from the other irrelevant tasks. Basic modules of the model developed for these purposes are explained below.

4.5.1. Integrator Module

This module implements the explicit integrator methods defined in the sections 4.2.1 through **??** . At the beginning, options of the module such as the method of integration, time step, start and final time of the simulation are input. If the integration method is not a self starting method rather a multistep method, lower order methods are also input in case the defaults are desired to be overridden.

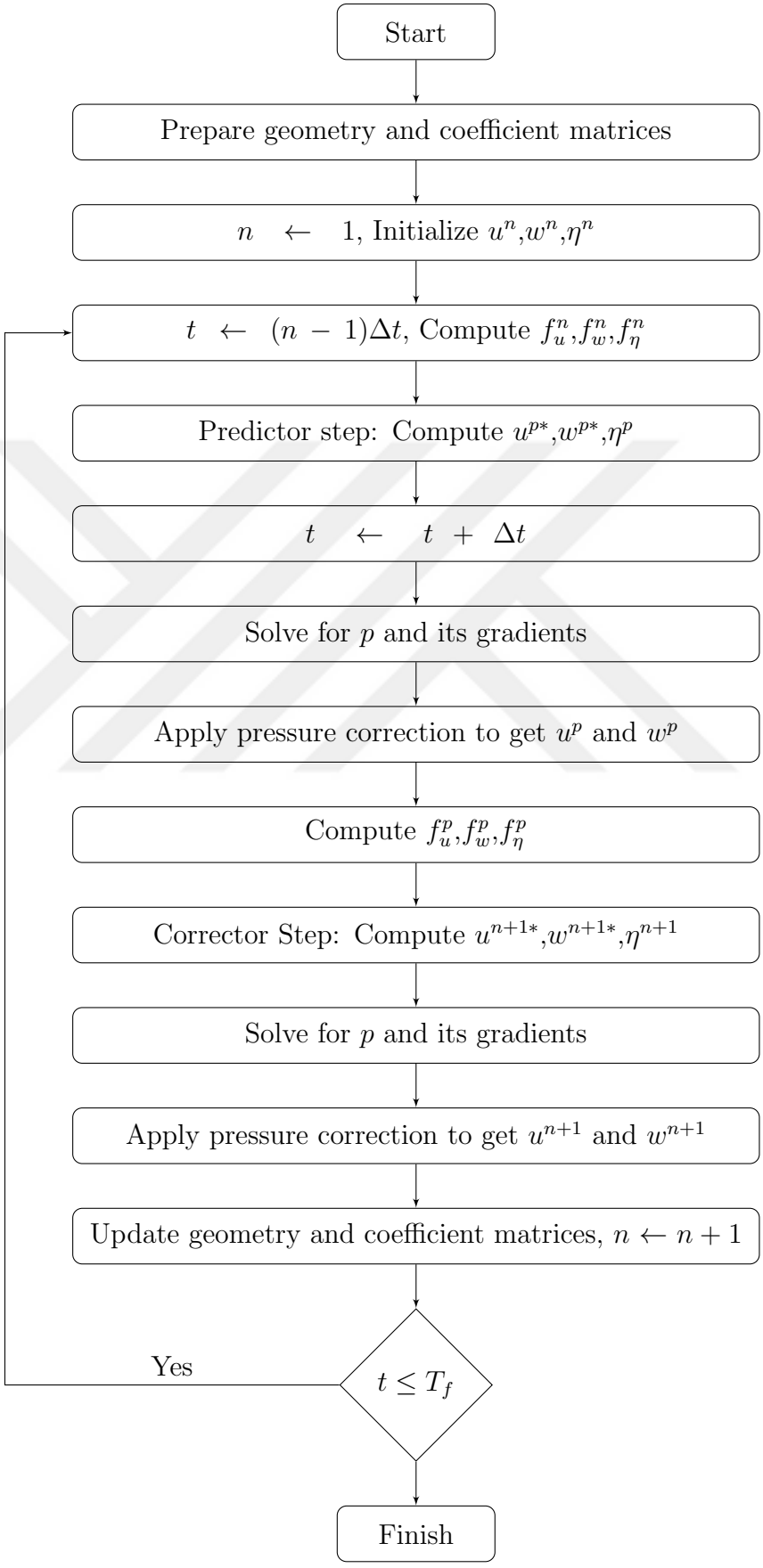

Figure 4.2. Sequential flow chart of the model

Another aspect of the module is that multiple variables in arrays of different sizes can be integrated through high level data types. This way the free surface in the size of the number of centers on the surface boundary can be integrated together with the velocity components in the size of the number of centers throughout the domain.

Also, depending on the free surface some of the centers inside the domain at a time step may fall outside the domain at a later time or the opposite may happen. Therefore, this method integrates the variables defined in the arrays through instantaneously updated ranges where centers out of these ranges are ignored. However this approach needs one other array that holds the history of the centers for the multistep methods since the centers freshly entering in the computations may need to be integrated with lower order methods until the main method of integration is possible to use.

This module is applicable to any kind of initial value problems since the routine computing the problem specific derivatives is provided through late-binding which is possible by a procedure pointer.

4.5.2. Geometry Module

This module manages the creation of the collocation centers and determination of the ranges of centers in use. The collocation centers are managed through collections in which centers are separated in groups. Therefore, it is easier to compute the valid range set at a time step. Also, using ranges performs better than performing computations on centers one-by-one.

4.5.3. Collocation Module

Once the geometry is set up this module performs the computation of coefficient matrices. Also, since the positions of the free surface change in time, coefficient matrices are updated accordingly with this module.

4.6. Stability and Filtering

For time dependent problems instabilities may occur in time in numerical models. Main treatment for the stabilization of the model is made by the PDE collocation on the boundary method as described above. However, due to nonlinear nature of the problem further smoothing is needed to filter out the unwanted noise that accumulates in time due to truncation of the floating point numbers. Therefore, 9 center Shapiro filter of Shapiro (1970) is used at some defined number of intervals during the computations on the surface centers. A 9 center Shapiro filter using 4 centers to the left and 4 centers to the right of the point of interest is used in the model. If there are m centers on the surface, values of the variable v at center i is as follows.

$$v_i^f = \frac{1}{256}\big[186v_i + 56\,(v_i + v_{i-1}) - 28\,(v_{i-2} + v_{i+2}) + 8\,(v_{i-3} + v_{i+3}) - (v_{i-4} + v_{i+4})\big] \tag{4.32}$$

On the other hand, since at the ends of the domain there are centers that do not have enough number of centers to use the given 9 center Shapiro filter, 3, 5 and 7 order filters are used for the three centers other than the ones at the ends. The values at the ends are left as they are. The 3, 5 and 7 center filters are respectively as follows.

$$v_i^f = \frac{1}{4}\big[2v_i + v_{i+1} + v_{i-1}\big] \tag{4.33}$$

$$v_i^f = \frac{1}{16}\big[10v_i + 4(v_{i+1} + v_{i-1}) - (v_{i-2} + v_{i+2})\big] \tag{4.34}$$

$$v_i^f = \frac{1}{64}\big[44v_i + 15(v_{i+1} + v_{i-1}) - 6(v_{i-2} + v_{i+2}) + v_{i-3} + v_{i+3}\big] \tag{4.35}$$

The filters presented here are symmetric as identical number of centers are used in the filters for both sides of the center of interest. There are unsymmetric filters using

different number of centers but they are not considered in this study.

5. TEST RESULTS

In this section, results of the validity tests are presented. Three waves of different depths are determined and used as an input. Their parameters and required values in time as the simulations proceed in time are computed using Stream Functions.

In the first part of the tests long duration (20 wave periods) tests are performed for horizontal bottom geometry with periodic boundary condition at the outgoing boundary. And the results are compared with the stream function wave form expected downstream. These tests are performed using the multi-quadric radial basis function that requires a shape parameter. Therefore, the process involving the determination of the optimum shape parameter is also presented.

In the second part of the tests, submerged break water test results are given and compared with the results of the experimental results of Luth et al. (1994).

The input waves used in the computations are selected from different water depths, namely deep, intermediate or shallow water. And their properties are given in Table 5.1.

Table 5.1. Properties of the input waves

Wave Name	Wave 1	Wave 2	Wave 3
Local Depth	0.4m	10m	5m
Period	2.02s	3s	15s
Height	0.02m	0.1m	0.1m
Length	3.74m	14.05m	103.5m
H/L	0.0053	0.0071	0.001
d/L	0.11	0.71	0.001
Depth	Intermediate	Deep	Shallow

Table 5.2. Summary of the test properties for the horizontal bottom simulations

Test Property	Integrator	RBF	Δt(s)	dx-dz(m)	nx-nz
Wave 1	ABM5	MQ	0.01	0.1-0.05	38-9
Wave 2	ABM5	MQ	0.01	0.41-0.25	35-41
Wave 3	ABM5	MQ	0.01	0.74-0.50	141-11

5.1. Horizontal Bottom Tests

For each of the waves defined in Table 5.1, a domain of one wavelength in the horizontal is assumed along with the local depth. Initially, the wave form is present in the domain which can be called a warm starting simulation. On the radiation boundary periodic boundary condition is used.

In all of the tests, MQRBF is used where the shape parameter is in the form of a factor. The integrator method selected is the Adams-Bashforth-Moulton Predictor Corrector Method of Order 5(ABM5). Time increment is 0.01s for all of the tests. Since the geometries differ for a given input wave, different number of centers are defined for each of the wave domains. Along the horizontal, 38 centers per wavelength are located for Wave 1 whereas 35 and 141 centers are located for Wave 2 and Wave 3. Similarly, 9, 41 and 11 centers are located in the vertical for each of the horizontal locations. Stream function solutions are computed using the Fenton (1988) numerical model. For each of the tests MQRBF is used where the shape parameter is in the form of a factor. The test configurations are summarized in Table 5.2.

5.1.1. Determination of Optimum Shape Parameter For The Waves

For each of the waves, several test runs are performed for 20 wave periods (T) with different values of the shape parameter and comparing with the stream function solution the root mean square errors are plotted with respect to these values in the Figures 5.1, 5.2 and 5.3. In these tests, number of centers is kept constant as given in Table **??** for a given wave. The shape parameters are in the form of a factor of

the distance term in the RBF expressions. Also, for the optimum shape parameters, variation of the root mean square errors are plotted in the Figures 5.4,5.4 and 5.4. It can be observed that Wave 1 deviates from the stream function solution of the potential theory by 1.6%, Wave 2 deviates 2.1% and Wave 3 deviates 0.9% of the wave height (H).

The resulting free surfaces during the first, tenth and twentieth periods at four instants are plotted in Figures 5.7, 5.8,5.9 for Wave 1, 5.10,5.11, 5.12 for Wave 2 and 5.13, 5.14, 5.15 for Wave 3. It is observed that the results are in good agreement with the expected surfaces.

5.2. Submerged Breakwater Test

For this test, experimental set up of Luth et al. (1994) illustrated in the Figure 5.16 is used. Compared to the original setup, instead of the beach, a sponge layer between horizontal locations $x = 25m$ and $x = 40m$ is used instead of the beach. At the end of the sponge layer, Sommerfeld radiation boundary condition is imposed to minimize the reflections. The reason for using a sponge layer is because of its simplicity because the beach requires a run-up, breaking and post-breaking model additional to the propagation model developed in the study.

For comparison purposes a fully nonlinear potential model is also developed and its results are presented along with the Navier-Stokes model. This has made it possible to compare two different numerical models of different theories. The results presented here are not the best match and no further simulations are performed to present the best match as the phenomena involved in the problem is complex. It can observed that the results are in agreement with the experimental results where there is some phase and amplitude difference between the results. These variations in the amplitude and the phase are because of the damping layer settings of the numerical models and beach setup of the experiment.

Ideally, the water surface is calm at the beginning, $t = t_0$ and if the simulations

continues long enough a steady profile can be observed. However, the simulations are cut after some time when the profiles resemble each other because there are no treatments for the reflection from the sponge layer and the breakwater in the setup.

At stations $x = 5.2m$, $x = 12.5m$, $x = 14.5m$ and $x = 17.3m$, the results of nonlinear potential theory model introduced in Appendix A is compared with the Navier-Stokes model developed for this study in the Figures 5.17, 5.18, 5.19, 5.20. And finally, both numerical model results are compared with the experiment results in the Figures 5.21, 5.22, 5.23 and 5.24.

At station $x = 5.2m$, the three profiles are almost identical. At station $x = 12.5m$ and $x = 14.5m$, the experimental results and nonlinear potential theory results are closer to each other compared to NSE results. However, at station $x = 17.3m$ experimental results and the NSE results are closer to each other while the potential theory results fall a little far from both of these result sets.

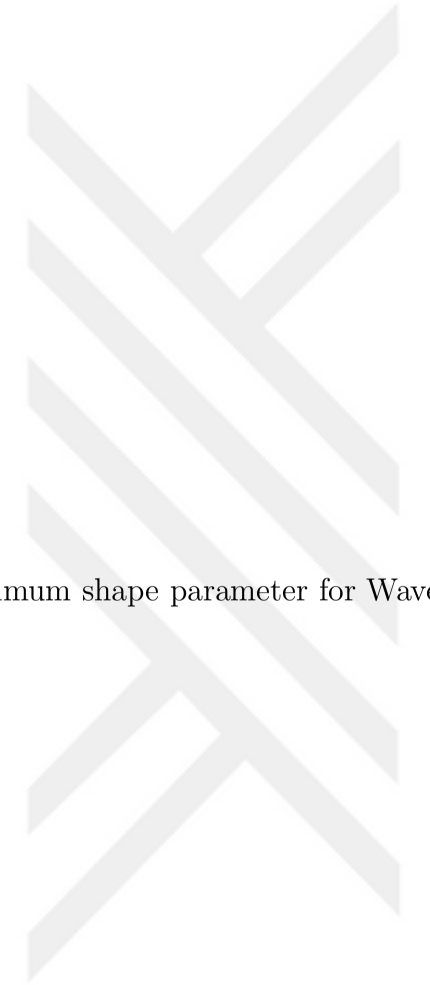

Figure 5.1. Determination of the optimum shape parameter for Wave 1.

Figure 5.2. Determination of the optimum shape parameter for Wave 2.

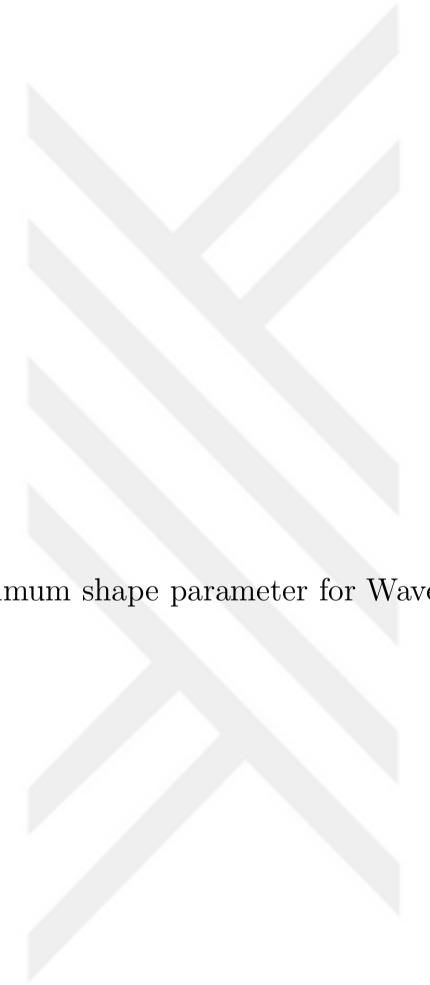

Figure 5.3. Determination of the optimum shape parameter for Wave 3.

Figure 5.4. Change of root mean square error in time for Wave 1.

Figure 5.5. Change of root mean square error in time for Wave 2.

Figure 5.6. Change of root mean square error in time for Wave 3.

Figure 5.7. Free Surface During The First Period For Wave 1.

Figure 5.8. Free Surface During The Tenth Period For Wave 1.

Figure 5.9. Free Surface During The Twentieth Period For Wave 1.

Figure 5.10. Free Surface During The First Period For Wave 2.

Figure 5.11. Free Surface During The Tenth Period For Wave 2.

Figure 5.12. Free Surface During The Twentieth Period For Wave 2.

Figure 5.13. Free Surface During The First Period For Wave 3.

Figure 5.14. Free Surface During The Tenth Period For Wave 3.

Figure 5.15. Free Surface During The Twentieth Period For Wave 3.

Figure 5.16. Setup of Luth et al. (1994) experiment.

Figure 5.17. Navier-Stokes and Nonlinear Potential model results at station $x = 5.2m$ for Wave 1.

Figure 5.18. Navier-Stokes and Nonlinear Potential model results at station $x = 12.5m$ for Wave 1.

Figure 5.19. Navier-Stokes and Nonlinear Potential model results at station $x = 14.5m$ for Wave 1.

Figure 5.20. Navier-Stokes and Nonlinear Potential model results at station $x = 17.3m$ for Wave 1.

Figure 5.21. Comparison of NS and Nonlinear Potential model results with the experiment at station $x = 5.2m$ for Wave 1.

Figure 5.22. Comparison of NS and Nonlinear Potential model results with the experiment at station $x = 12.5m$ for Wave 1.

Figure 5.23. Comparison of NS and Nonlinear Potential model results with the experiment at station $x = 14.5m$ for Wave 1.

Figure 5.24. Comparison of NS and Nonlinear Potential model results with the experiment at station $x = 17.3m$ for Wave 1.

6. CONCLUSION

This study shows that based on the Navier-Stokes mathematical model, water wave propagation can be modeled with radial basis function collocation method and the model developed in the study can be used for the estimation of wave parameters in the flow field. Considering the flexibility, accuracy and ease of development that RBFCM provides, it is also shown that more complex flows in more challenging conditions can be modeled with more realistic mathematical assumption of water wave propagation phenomenon.

In the future studies, the model can be coupled with a turbulence model to account for the imperfections in the problem geometry. Also, already built-in three dimensional module can be verified with 3D benchmark tests. A turbulence model estimates the thickness of the boundary layer and gives an estimate for the viscosity which can be incorporated into the model through the viscous term that has the kinematic viscosity as a coefficient. Further, this will bring the necessity of using different implementations at the inside and outside of the boundary layer.

Another follow up study can be the implementation of wave breaking into the model. Since some of the RBF centers are collocated like particles on the free surface, it will not be too much difficult to overcome the multiple-valuedness problem when the waves start to overturn for some breaking types. This extension also requires an implementation of dissipation mechanism on the surface and flow definition after breaking.

Since the model is developed in modules, it is also possible to use some of them to develop solvers for other type of flows. Solvers will only determine the locations of the collocation centers, input the initial values and modify the parameters in time according to the boundary conditions of the flow problem being modeled.

REFERENCES

Agnon, Y., Madsen, P. A. and Schäffer, H. A., 1999, "A new approach to high-order Bussinesq models", *Journal Fluid Mechanics*, Vol. 399, pp. 319-333.

Airy, G., 1845, "Tides and Waves", *Encyclopedia Metropolitana*.

Alfrink, B.J. and Rijn, L.C. van, 1983, "Two-Equation Turbulence Model for Flow in Trenches", *Journal of Hydraulic Engineering*, Vol. 109(7),pp. 941-958.

Benjamin, T. B., Bona, J. L. and Mahony, J. J., 1972, "Model equations for long waves in non-linear dispersive systems", *Phil. Trans. Roy. Soc. Lond. A*, Vol 272, pp. 47-48.

Berkhoff, J.C.W., 1972, "Computation of combined refraction and diffraction", *Proceedings of the 13th International Coastal Engineering Conference*, ASCE, pp. 569-587.

Berkhoff, J.C.W., 1976, *Mathematical models for simple harmonic linear water waves; wave refraction and diffraction*, Ph. D. Thesis, Delft Technical University of Technology.

Boussinesq, J., 1872, "Theorie des onde et des resous qui se propagent le long d'un canal rectangulaire horizontal, en communiquant au liquide contenu dans ce canal des vitesses sensiblement pareilles de la surface au fond",*Journal de math. Pures et Appl., Deuxieme Serie*, Vol. 17, pp. 55-108.

Brocchini, M., Drago, M. and Iovenitti, L., 1992, "The modeling of short waves in shallow waters. Comparison of numerical models based on Boussinesq and Serre equations", *ASCE Proc. 23rd Int. Conf. Coastal Engrg.*, pp. 76-88.

Brocchini, M., 2013, "A reasoned overview on Boussinesq-type models: the inteplay be-

tween physics, mathematics and numerics", *Proc Roy Soc A*, 469(2160):20130496.

Broeze, M., 1993, "Numerical modeling of nonlinear free surface waves with a 3D panel method", *Ph. D. Thesis*, University of Twente, Twente, The Netherlands.

Burden, R.L, and Faires, J.D., 2011, *Numerical Analysis*, 9th Ed., Brooks/Cole, Boston.

Cebeci, T., 2004, *Turbulence Models and Their Application Efficient Numerical Methods with Computer Programs*, Horizons Publishing, Long Beach.

Cebeci, T., Shao, J. P., Kafyeke, F., Laurendeau, E., 2005, *Computational Fluid Dynamics For Engineers*, Horizons Publishing, Long Beach.

Chappelear, J. E., 1961, "Direct numerical calculation of wave properties", *J. Geophys. Res.*, Vol. 66(2), pp. 501–508.

Chen, W., 2002, *New RBF collocation schemes and kernel RBFs with applications*, Lect. Notes Comput. Sci. Eng., Vol. 26, pp. 75–86.

Chen, W., Fu, Z-J., Chen, C.S., 2014, *Recent Advances in Radial Basis Function Collocation Methods*, Springer Heidelberg, New York.

Chen Q., Madsen P.A., Schäffer, H. A., Basco, D. R., 1998, "Wave-current interaction based on an enhanced Boussinesq approach", *Coastal Engrg.*, Vol. 33, pp. 11-39.

Chorin, A. J., 1968, "Numerical solution of the Navier-Stokes equations.", *Math. of Computation*, 22, 745–762.

Courant, R., Friedrichs, K., Lewy, H., 1928,"Über die partiellen Differenzengleichungen der mathematischen Physik", *Mathematische Annalen* (in German), Vol. 100(1), pp. 32-74.

Dean, R., 1965, "Stream Function Representation of Nonlinear Ocean Waves", *J. Geophys. Res.*, Vol. 70, pp. 4561-4571.

Dean, R. G., 1974, "Evaluation and Development of Water Wave Theories for Engineering Application Vol.1 and 2. Spec. Rep. 1" , Tech. rep., Coastal Engineering Research Center, Fort Belvoir, Va.

Dean, R. G. and Dalrymple, R. A., 1984, *Water Wave Mechanics for Engineers and Scientists*, Prentice-Hall Inc., Englewood Cliffs, New Jersey.

Dingemans, M. W., 1997a, *Water Wave Propagation Over Uneven Bottoms:Part 1–Linear Wave Propagation*, World Scientific Publishing, Singapore.

Dingemans, M. W., 1997b, *Water Wave Propagation Over Uneven Bottoms:Part 2–Non-linear Wave Propagation*, World Scientific Publishing, Singapore.

Duchon, J., 1977, "Splines Minimizing Rotation-Invariant Semi-Norms in Sobolev Spaces, Constructive Theory of Functions of Several Variables", *Lecture Notes in Mathematics*, Springer, Vol.571, pp.85-100.

Eckart, C., 1952, "The propagation of gravity waves from deep to shallow water.", Circular 20, *National Bureau of Standards*, pp. 165-173.

Eringen, C., 1980, *Mechanics of Continua*, Robert E. Krieger Publishing, New York.

Fedoseyev, A.L., Friedman, M.J., Kansa, E.J., 2002, "Improved multiquadric method for elliptic partial differential equations via PDE collocation on the boundary", *Comput. Math. Appl.*, Vol. 43(3–5), pp. 439–455.

Fenton, J. D., 1985, "A Fifth-Order Stokes Theory for Steady Waves", *ASCE Jour. Waterw., Port, Coastal and Ocean Engr.*, Vol. 111, pp. 216-234.

Fenton, J.D., 1988, "The Numerical Solution of Steady Water Problems", *Computers & Geosciences*, Vol.14, No. 3, pp. 357-368.

Ferziger, J.H. and Peric, M, 2002, *Computational Methods for Fluid Dynamics*, Springer Verlag, Berlin Heidelberg New York.

Flyer, N., Wright, G.B., Fornberg, B., 2015, Radial Basis Function-Generated Finite Differences: A Mesh-Free Method for Computational Geosciences, *Handbook of Geomatics: Second Edition*, pp. 2635-2669.

Fornberg, B., Flyer, N., 2015, *A Primer on Radial Basis Functions with Applications to the Geosciences*, E-book, Society for Industrial and Applied Mathematics.

Fornberg, B., Lehto, E., Powell, C., 2013, "Stable Calculation of Gaussian-based RBF-FD stencils", *Comput. Math. Appl.*, Vol. 65(4), pp. 627-637.

Franke, R., 1982, "Scattered data interpolation: Test of Some Methods", *Mathematics of Computation*, Vol. 38, No. 157, pp. 181-200.

Gobbi, M. F., Kirby, J. T., 2000, "Wave evolution over submerged sills: test of high order Boussinesq model", *Coastal Engrg*, Vol. 37, pp. 57-96.

Gobbi, M. F., Kirby, J. T., Wei, G., 2000, "A fully nonlinear Boussinesq model for surface waves. Part 2. Extension to $O(kh)^4$", *J. Fluid Mech.*, Vol. 405, pp. 181-210.

Hardy, R.L., 1971, "Multiquadric equations of topography and other irregular surfaces", *Journal of Geophysical Research*, Vol. 76(26), pp. 1905-1915.

Harlow, F.H. and Welch J.E., 1965, "Numerical Calculation of Time-Dependent Viscous Incompressible Flow of Fluid with Free Surface", *The Physics of Fluids*,Vol. 8(12), pp. 2182-2189.

Hirt, C.W., Amsden, A.A. and Cook, J.L., 1974, "An arbitrary Lagrangian-Eulerian computing method for all flow speeds", *J. Comput. Phys.*, Vol. 14, pp. 227-253.

Hirt, C.W. and Nichols, B.D., 1981, "Volume of Fluid (VOF) Method for the Dynamics of Free Boundaries", *J. Comput. Phys.*, Vol. 39, pp. 201-225.

Isreali, M., Orszag, S., 1981, "Approximation of radiation boundary condition",*Journal*

of Computational Physics,pp. 115-135.

Issa, R. I. and Lockwood, F. C., 1977, "On the Prediction of Two-dimensional Supersonic Viscous Interactions near Walls", *AIAA J.*, Vol. 15, No. 2, pp. 182–188.

Kaihatu, J. M., 2003, "Frequency domain wave models in the nearshore and surfzones", In: Advances in coastal modeling (Lakhan, V.C. ed.), Vol. 67, pp. 43-72, Elsevier Oceanography Series.

Kanoğlu, U., 2004, "Nonlinear evolution and runup-rundown of long waves over a sloping beach", *J. Fluid Mech.*, Vol. 513, pp. 363–372.

Kansa, E.J., 1990a, "Multiquadrics - A Scattered Data Approximation Scheme with Applications to Computational Fluid Dynamics-I Surface Approximations and Partial Derivative Estimates", *Computers and Mathematics with Applications*, Vol. 19, No. 8/9, pp. 127-145.

Kansa, E.J., 1990b, "Multiquadrics- A Scattered Data Approximation Scheme with Applications to Computational Fluid Dynamics-II Solutions to Parabolic, Hyperbolic and Elliptic Partial Differential Equations", *Computers and Mathematics with Applications*, Vol. 19, No. 8/9, pp. 147-161.

Karambas, T. and Koutitas, C., 1992, "A breaking wave propagation model based on the Boussinesq equations", *Cosatal Engrg.*, Vol. 18, pp. 1-19.

Kennedy, A.B., Fenton, J.D., 1996, "A Fully Nonlinear 3D Method for the Computation of Wave Propagation", *Proceedings of the 25th International Conference on Coastal Engineering*, pp. 1102-1115.

Kennedy, A.B. and Fenton, J.D., 1997, "A fully-nonlinear computational method for wave propagation over topography", *Coastal Engineering*, pp. 137-161.

Kennedy, A. B., Chen, Q., Kirby, J. T. and Dalrymple, R. A., 2000, "Boussinesq

modeling of wave transformation, breaking and runup. I: 1D", *J. Waterway, Port, Coastal and Ocean Engineering*, Vol. 126, pp. 206-214.

Kirby, J.T. and Dalrymple, R.A., 1983, "A parabolic equation for the combined refraction-diffraction of Stokes waves by mildly varying topography",*J.Fluid Mech.*, Vol. 136, pp. 543-566.

Kirby, J. T., 1997, "Nonlinear dispersive long waves in water of variable depth, In: Gravity waves in water of finite depth (Hunt, J. N. ed.), *Advances in Fluid Mechanics*, Vol.10, pp. 55-125, Comp. Mech. Publications.

Kirby, J. T., 2003, "Boussinesq models and applications to nearshore wave propagation surf zone processes and wave induced currents", In: Advances in coastal modeling (Lakhan, V.C. ed.), Vol. 67, pp. 1-42, Elsevier Oceanography Series.

Korteweg, D. and G. de Vries, 1895, "On the Change of Form of Long Waves Advancing in a Rectangular Channel, and on New Type of Long Stationary Waves", *Philos. Mag. Series 5* , Vol. 39(240), pp. 422-443.

Kowalik, Z. and Murty, T.S., 1993, *Numerical Modeling of Ocean Dynamics*, World Scientific Publishing, Singapore.

Kupradze, V.D., Aleksidze, M.A., 1964, "The method of functional equations for the approximate solution of certain boundary value problems", *USSR Comput. Math. Math. Phys.* 4(4), 82–126.

Launder, B. E. and Spalding, D. B., 1974, "The Numerical Computation of Turbulent Flows", *Comput. Methods Appl. Mech. Eng.*, Vol. 3, pp. 269–289.

Le Méhauté, B., 1976, *Introduction to Hydrodynamics and Water Waves*, Springer-Verlag, New York.

Li, B., 2008, "A 3-D model based on Navier-Stokes equations for regular and irregular

water wave propagation", *Ocean Engineering*, Vol. 35, pp. 1842-1853.

Li, B. and Fleming, C.A., 1997, "A three dimensional multigrid model for fully non-linear water waves", *Coastal Engineering*, Vol. 30, pp. 235-258.

Li, B. and Fleming, C.A., 2001, "Three-Dimensional Model of Navier-Stokes Equations for Water Waves", *J. Waterw. Port Coastal Ocean Eng.*, Vol. 127(1), pp. 16-25.

Lin, P. and Li, C.W., 2002, "A σ-coordinate three-dimensional numerical model for surface wave propagation", *Int. J. Numer. Meth. Fluids*, Vol. 38, pp. 1045-1068.

Liu, P. L.-F., Cho, Y.S., Briggs, M. J., Kanoğlu, U. and Synolakis C.E., 1995, "Runup of solitary waves on a circular island", *J. Fluid Mech.*, Vol. 302, pp. 259–285.

Longuet-Higgins, M.S. and Cokelet, E.D., 1976, "The deformation of steep surface waves on water I. A numerical method of computation", *Proceedings of the Royal Society of London. A*, Vol. 350, pp. 1-26, July.

Luth, H., Klopman, G., and Kitou, N., 1994, "Projects 13G: Kinematics of waves breaking partially on an offshore bar: LVD measurements for waves without a net onshore current.", *Technical Report H1573*, Tech. rep., Delft Hydraulics.

Ma G., Shi F. and Kirby J.T., 2012, "Shock-capturing non-hydrostatic model for fully dispersive surface wave processes", *Ocean Modelling*, Vol. 43-44, pp. 22-35.

Ma, Q. ed., 2010, *Advances in Numerical Simulation of Nonlinear Water Waves*, Advances In Coastal and Ocean Engineering Volume 11, Singapore: World Scientific Publishing, 690 p.

Madsen, P. A., Murray, R. and Sørensen, O. R., 1991, "A new form of the Boussinesq equations with improved linear dispersion characteristics. Part 2. A slowly-varying bathymetry", *Coast. Engrg.*, Vol. 18, pp. 183-204.

Madsen, P. A. and Schäffer, 1998, "Higher-order Boussinesq-type equations for surface

gravity waves: derivation and analysis", *Phil. Trans. R. Soc. Lond. A*, Vol. 356, pp. 3123-3184.

Madsen, P. A., Bingham, H. B., Liu, H., 2002, "A new Boussinesq model for fully nonlinear waves from shallow water to deep water", *J. Fluid Mech.*, Vol. 462, pp. 1-30.

Madsen, P.A., Bingham, H. B., Schäffer, H. A., 2003, "Accuracy and convergence velocity formulations for water waves in the fraamework of Boussinesq theory", *J. Fluid Mech.*, Vol. 477, pp. 285-319.

Mei, C.C., 1983, *The Applied Dynamics of Ocean Surface Waves*, World Scientific Publishing, Singapore.

Menter, F. R., 1992a, "Performance of Popular Turbulence Models for Attached and Separated Adverse Pressure Gradient Flow", *AIAA J.*, Vol. 30, pp. 2066–2072.

Menter, F. R., 1992b, *Improved Two-equation $k-\omega$ Turbulence Models for Aerodynamic Flows*, NASA Technical Memorandum TM 103975, NASA Ames, CA.

Menter, F., 1994, "Two-equation Eddy-viscosity Turbulence Model for Engineering Applications", *AIAA J.*, Vol. 32, pp. 1598–1605.

Menter, F., 1997, "Eddy-viscosity Transport Equations and their Relation to the k–ϵ Model", *Trans. ASME, J. Fluids Eng.*, Vol. 119, pp. 876–884.

Miller, M.J., and Thorpe, A.J. (1981),"Radiation conditions for the lateral boundaries of limited-area numerical models",*Quarterly J. Royal Meteorological Society*, Vol. 107, pp. 615-628.

Monaghan, J.J., 1992, "Smoothed Particle Hydrodynamics", *Annu. Rev. of Astron. Astrophys.*, Vol. 30, pp. 543-574.

Munk, 1949, W. H., "The Solitary Wave Theory and Its Applications to Surf Zone

Problems", *Ann. N. Y. Acad. Sci.*, Vol. 51, pp 376-424.

Nwogu, O., 1993, "An alternative form of Boussinesq equations for nearshore wave propagation",*Journal of Waterway, Port, Coastal Ocean Engineering, ASCE*, Vol. 119, pp. 618-638.

Osher, S. and Sethian, J. A., 1988, "Fronts propagating with curvature-dependent speed: Algorithms based on Hamilton–Jacobi formulations", *J. Comput. Phys.*, Vol. 79, pp. 12–49.

Patankar, S. V., 1980, *Numerical Heat Transfer and Fluid Flow*, Hemisphere Publishing Corporation, Taylor and Francis Group, New York.

Patankar, S. V. and Spalding, D. B., 1972, "A Calculation Procedure for Heat, Mass and Momentum Transfer in Three-dimensional Parabolic Flows", *Int. J. Heat Mass Transfer*, Vol. 15, pp. 1787-1806.

Peregrine, J., 1967, "Long waves on a beach, *J Fluid Mech.*, Vol. 27, No. 4, pp. 815-827.

Press, W. H., Flannery, S., Teukolsky, A. and Wetterling, W. T., 1986, *Numerical Recipes*, Cambridge University Press.

Rienecker, M.M. and Fenton J.D., 1981, "A Fourier approximation method for steady water waves", *Jour. Fluid Mech.*, Vol. 104, pp. 119-137.

Romate, J.E., 1989, "The numerical simulation of nonlinear gravity waves in three dimensions using a higher order panel method", *Ph.D. Thesis*, Delft Hydraulics.

Schäffer, H. A., Madsen, P. A. and Deigaard, R., 1993, "A Boussinesq model for waves breaking in shallow water", *Coastal Engrg.*, Vol. 29, pp. 185-202.

Serre P. F., 1953, "Contribution á l'étude des écoulement permanents et variables dans les canaux", *La Houille Blanche*, pp. Vol. 8 (6-7),374-488; Vol. 8(12), pp. 830-872.

Schlichting, H., 1979, *Boundary-Layer Theory*, McGraw Hill, New York.

Shapiro, R., 1970, "Smoothing, filtering, and boundary effects", *Reviews of Geophysics*, Vol. 8(2), pp. 359-387.

Sobey, R. J., Goodwin, P., Thieke, R.J. and Westberg, R.J., 1987, "Application of Stokes, cnoidal, and Fourier wave theories", *J. Waterway Port Coastal and Ocean Engnrng*, Vol. 113, pp. 565-587.

Sommerfeld, A., 1949, *Partial differential equations in physics*, Academic Press, New York.

Speziale, C. G., 1987, "On Non-linear k–l and k–ϵ Models of Turbulence:", *J. Fluid Mech.*, Vol. 178, pp. 459–475.

Stoker, J. J., 1957, *Water Waves, The Mathematical Theory with Applications*, Interscience, New York.

Stokes, G., 1847, "On the Theory of Oscillatory Waves", *Trans. Camb. Philos. Soc.*, Vol. 8, pp. 441-455.

Svendsen, I. A., 2006, *Introduction to Nearshore Hydrodynamics*, World Scientific Publishing, Singapore.

Synolakis, C.E., 1987,"The runup of solitary waves", *J. Fluid Mech.*, Vol. 185, pp. 523-545.

Thacker, W.C., 1981, "Some Exact Solutions to the Nonlinear Shallow-Water Wave Equations", *J. Fluid Mech.*, Vol. 107, pp. 499-508.

Temam, R., 1969, "Projection methods for solving sparse linear systems.",*The Comp. J.*, Vol.12(1), pp. 77–80.

Titov, V. V. and Synolakis, C.E., 1997, "Extreme inundation flows during the Hokkaido-

Nansei-Oki Tsunami", *Geophys. Res. Lett.*, Vol. 24(11), pp. 1315–1318.

Tsay, T.-K. and Liu, P.L.-F., 1982,"Numerical solution of water wave refraction and diffraction problems in the parabolic approximation",*J. Geophys. R.*, Vol. 87 (C10), pp. 7932-7940.

Ursell, F., 1953, "The Long-Wave Paradox in the Theory of Gravity Waves", emphProc. Camb. Philos. Soc., Vol. 49, pp. 685-694.

Van Doormal, J. P. and Raithby, G. D., 1984, "Enhancements of the SIMPLE Method for Predicting Incompressible Fluid Flows", *Numer. Heat Transfer*, Vol. 7, pp. 147–163.

Veeramony, J. and Svendsen, I. A., 1998, "A Boussinesq model for surf zone waves: Comparison with experiments", *Proc. 26th Intl. Conf. Coastal Engrg.*, pp. 258-271.

Veeramony, J. and Svendsen, I. A., 2000, "The flow in the surf zone waves", *Coastal Engrg.*, Vol. 39, pp. 93-122.

Versteeg, H. K., Malalasekera, W., 2007, *An Introduction to Computational Fluid Dynamics*, 2nd ed., Pearson Education Limited, Essex.

Wei, G. and Kirby, J. T., 1995, *A time dependent numerical code for extended Boussinesq equations*, Newark, Del, University of Delaware, Dept. of Civil Engineering, Center for Applied Coastal Research.

Wei, G., Kirby, T., Grilli, S. T. and Subramanya, R., 1995, "A fully nonlinear Boussinesq model for surface waves. Part I. highly nonlinear unsteady waves", *J. Fluid Mech.*, Vol. 294, pp. 71-92.

Wendland, H., 1995, "Piecewise Polynomials, Positive Definite and Compactly Supported Radial Basis Functions of Minimal Degree", *Advances in Computational*

Mathematics, Vol. 4, pp. 389-396.

Wertz, J., Kansa, E.J., Ling, L., 2006 "The role of the multiquadric shape parameters in solving elliptic partial differential equations',*Comput. Math. Appl.*, Vol. 51(8), pp. 1335–1348.

Whitham, G. B., 1999, *Linear and Nonlinear Waves*, John Wiley and Sons, New York.

Wilcox, D. C.,1988, "Reassessment of the Scale-determining Equation for Advanced Turbulence Models", *AIAA J.*, Vol. 26, No. 11, pp. 1299–1310.

Wilcox, D. C.,1993a, "Comparison of Two-equation Turbulence Models for Boundary Layers with Pressure Gradients", *AIAA J.*, Vol. 31, No. 8, pp. 1414–1421.

Wilcox, D. C.,1993b, *Turbulence Modelling for CFD*, DCW Industries Inc., La Canada, CA.

Wilcox, D. C.,1994, "Simulating Transition with a Two-equation Turbulence Model", *AIAA J.*, Vol. 32, pp. 247–255.

Wong, A.S.M., Hon, Y.C., Li, T.S., Chung, S.L., Kansa, E.J., 1999, "Multizone decomposition for simulation of time-dependent problems using the multiquadric scheme", *Comput. Math. Appl.*, Vol. 37(8), pp. 23-43.

Yoon, S.B. and Liu, P. L.-F., 1989, "Interaction of currents and weakly nonlinear waves in shallow water", *J. Fluid Mech.*, Vol. 205, pp. 397-419.

Yuan, H. and Wu, C.H., 2004, "A two-dimensional vertical non-hydrostatic σ-model with an implicit method for free-surface flows", *Int. J. Numer. Meth. Fluids*, Vol.44, pp.811-835.

Zelt, J. A., 1991, "The runup of nonbreaking and breaking solitary waves", *Coastal Engrg.*, Vol. 15, pp. 205-246.

APPENDIX A: NONLINEAR POTENTIAL MODEL

Nonlinear potential model results are also displayed in the submerged breakwater test for comparison. Details of the mathematical and numerical model are presented here.

A.1. Mathematical Model

Based on the following assumptions

- The flow is unsteady.
- Incompressible.
- Fluid is inviscid.
- Flow is irrotational.
- Model verification cases are selected so that all of the wave properties and the physical conditions do not change in the transverse direction. Therefore, definitions and formulations are made in 2D. As it will be apparent in the next chapter where the numerical formulation of the problem and its implementation is presented, accounting for the 3D problems requires not more that the additional boundary conditions and more computer resources.
- Bottom boundary is rigid and impermeable.
- Density of the water is constant throughout the domain.

for a velocity potential function $\phi = \phi(x, z, t)$ defined throughout the domain such that

$$\frac{\partial \phi}{\partial x} = u \qquad \frac{\partial \phi}{\partial z} = w \tag{A.1}$$

where u and w are the velocity components, the equation of continuity, i.e.

$$\frac{\partial u}{\partial x} + \frac{\partial w}{\partial z} = 0 \tag{A.2}$$

reduces to the Laplace's equation

$$\nabla^2\phi = 0 \tag{A.3}$$

which valid over the problem domain. And the nonlinear kinematic and dynamic free surface boundary conditions on the free surface $z = \eta(x,t)$ respectively becomes.

$$\frac{\partial\eta}{\partial t} = \frac{\partial\phi}{\partial z} - \frac{\partial\phi}{\partial x}\frac{\partial\eta}{\partial x} \tag{A.4}$$

$$\frac{\partial\phi}{\partial t} = -g\eta - \frac{1}{2}|\nabla\phi|^2 + \frac{\partial\phi}{\partial z}\frac{\partial\eta}{\partial t} \tag{A.5}$$

The dynamic free surface boundary condition given in A.5 is based on semi-Lagrangian approach.

On the bottom $z = z_b(x)$,

$$\frac{\partial\phi}{\partial z} + \frac{\partial\phi}{\partial x}\frac{\partial z_b}{\partial x} = 0 \tag{A.6}$$

rigid impermeable boundary condition is valid. On the input boundary at $x = x_L$, wave parameters are known. If the outgoing boundary condition is periodic, it is assumed that wave properties are assumed to be equal to properties at the input boundary for integral distances of domain length. One of the two other boundary conditions is the Sommerfeld radiation boundary condition given as follows.

$$\frac{\partial\phi}{\partial t} + c\frac{\partial\phi}{\partial x} = 0 \tag{A.7}$$

And, according to the sponge boundary condition for $x_R \geq x \geq x_s$, the dynamic

free surface boundary condition is modified.

$$\frac{\partial \phi}{\partial t} = -g\eta - \frac{1}{2}|\nabla \phi|^2 - c_s(x)\phi \tag{A.8}$$

where x_s is the starting location of the sponge layer, $c_s(x)$ is the sponge coefficient.

A.2. Numerical Methodology

In this model, boundary conditions are time dependent while the governing equation in A.3 is steady. Therefore, the unknown variables are the free surface η, velocity potential ϕ on the surface and the velocity potentials on the outgoing boundary at $x = x_R$ if the Sommerfeld boundary condition is used. However, at an instant spatial the derivatives of the velocity potential is obtained by solving the boundary value problem for the potentials.

Also, PDE collocation on the boundary method is implemented in the model so that each of the boundary centers has a corresponding center just outside the domain to provide the necessary number of equations. Therefore, it is possible to define the governing equation in A.3 along with the boundary condition at each of the boundary centers. Therefore given N collocation centers defined over the domain M of which defined on the boundaries, an additional M collocation centers are defined outside the domain. The approximate definition for the velocity potential ϕ at center i is as follows.

$$\phi(\mathbf{x}_i, t) = \sum_{j=1}^{N+M} \alpha_j^{\phi} \varphi(|\mathbf{x}_i - \mathbf{x}_j|, \epsilon) \tag{A.9}$$

where $\mathbf{x}_i$ is the vector denoting the position of the center i, φ is a radial basis function which depends on the geometric distance between centers i and j, and ϵ is a shape parameter that may exist in the definition of a radial basis function. Magnitude of the shape parameter ϵ determines the flatness of the radial basis functions being used. Also, the spatial derivatives of the velocity potential are given below.

$$\frac{\partial \phi_i}{\partial x} = \sum_{j=1}^{N} \frac{\partial \varphi_{ij}}{\partial x} \alpha_j^{\phi} \qquad \frac{\partial \phi_i}{\partial z} = \sum_{j=1}^{N} \frac{\partial \varphi_{ij}}{\partial z} \alpha_j^{\phi} \qquad \nabla^2 \phi_i = \sum_{j=1}^{N} \nabla^2 \varphi_{ij} \alpha_j^{\phi} \tag{A.10}$$

On the other hand, the free surface variable η can be expressed similar to the Equation 4.30 and the spatial derivatives is identical to the derivatives expressed by the equations given in 4.31.

A.2.1. Program Flow

In this section sequential program flow is presented even the modules described in Section 4.5 are also used in the nonlinear potential theory model. From T_0 to T_f incrementing time by Δt at each time step, following steps are followed for a predictor-corrector type integration method.

(i) Centers over the domain along with the extra centers outside the domain are located. The coefficient matrices are prepared.

(ii) Unknown parameters ϕ^n, η^n are initialized for $n = 1$.

(iii) Time rate of change of the variables f_{ϕ}^n,f_{η}^n are computed using A.5, A.4.

(iv) Using the predictor step of the integrator method predicted values ϕ^p and eta^p are computed.

(v) Time is incremented by Δt.

(vi) Boundary value problem for the potentials given in Equation A.3 is setup and and solved for the potential coefficients α^{ϕ} given in A.9 and the required spatial derivatives are computed using A.10

(vii) Using the predicted values of the unknowns, rate of change of the variables are computed, i.e. f_{ϕ}^p and f_{η}^p are obtained.

(viii) ϕ^{n+1} and η^{n+1} for the new time step $n+1$ are computed using the corrector step of the integration method.

(ix) Geometry is updated using η^{n+1} and the coefficient matrices are updated accord-

ingly at the end of the time step.

(x) Steps (iii) to (ix) are repeated until the final time T_f is reached.

A flowchart of the steps described above is given in Figure A.1.

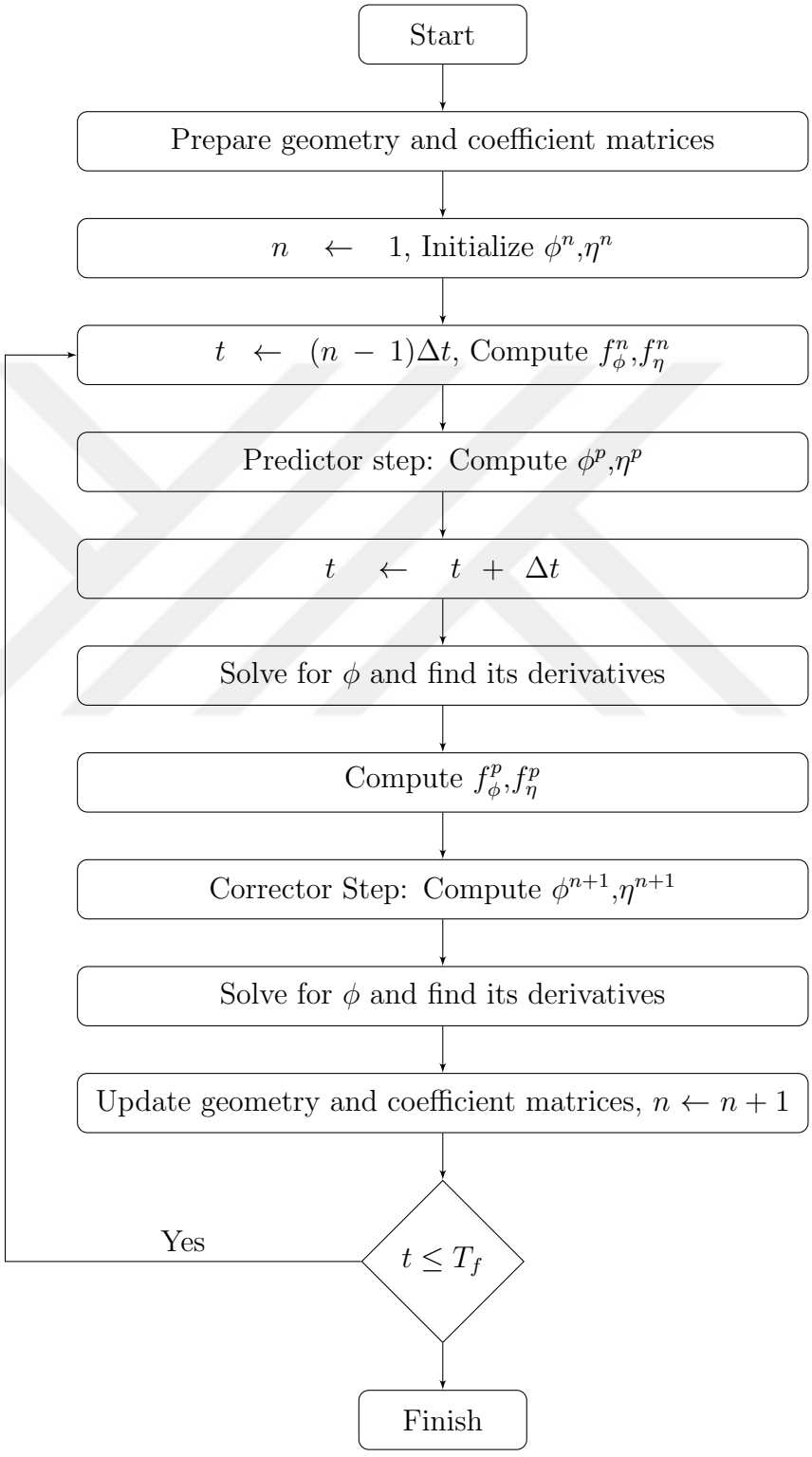

Figure A.1. Sequential flow chart of the model

APPENDIX B: SOURCES OF ERROR IN NUMERICAL MODELS

Numerical errors are inevitable in models and magnitude of them is one of the important parameters in validating accuracy of the results. There are several factors causing these errors which are very well known by seasoned modelers. Depending on its nature, errors may lie in a band around the target results, fluctuate with a pattern visible to an eye, sometimes propagate and sometimes grow in time for unsteady problems and iterative solutions. For a numerical modeler, it is important to keep the numerical errors under control to prevent inaccurate calculations. Sources of errors can be listed as such.

- Approximation of continuous unknowns in a discrete space.
- Complexity of the problem due to its definition or other geometric restraints.
- Insufficient problem definition, especially on boundaries.
- Rounding and truncation errors.
- Method errors.

Numerical models, basically, perform simultaneous solution of equation sets composed of discrete parameters that are defined as an approximate counterpart of the continuous parameters of the problem domain. This representation does not result in unexpected results if the target solution is smooth like the figure below however sometimes due to the nature of the problem steep changes may occur and might be local. As a precaution algorithms are developed to adapt these steep changes and pay much more attention than smooth regions. Also in some cases resolution of discretization might not be enough to catch the expected behavior. This is a very common issue for modelers whose problems involve turbulence.

Figure B.1. A continuous and a discrete sinosoidal function.

Another issue in the accuracy of numerical models is the complexity of the prob-

lems they can solve. Either the mathematical description contains complex terms like the viscous term in fluid models or the geometry can be very complex. Complex geometries are hard to discretize and define corresponding equation sets which are mostly a function of the problem geometry.

Sometimes available mathematical description of the problem might be insufficient and modelers try to construct a work around to handle the situation using artificial components, independent equations or representations. A common example to this error source is the radiation boundary conditions for elliptic wave propagation problems. There are well devised equations to overcome this difficulty for wave models truncating the problem domain. Eventually, these solutions all remain as approximate definitions.

Roundoff and truncation errors are more common error types, former of which depends on the storage capacity of computer systems and the latter is caused by chopping off the terms of a series expansion after some order. In computers, real type variable cannot be stored exactly binary representation of variable values are stored as much as it is possible by the capacity of the system. This may cause inaccurate calculations and catastrophic failures may occur like some reported events in the last decades.In the truncation error, since it is impossible to construct an infinite loop and since computation time is critical in some model runs, it is best to ignore the terms after some limit. This might cause problems if the terms neglected are considerable in magnitude.

And a final possible source of error worth to note is method specific errors. It depends on the type of discretization where discrete set of equations are defined to get approximations of parameters. For example, explicit time integration methods are well known to cause instabilities during the computations where most of the time Courant–Friedrichs–Lewy (CFL) condition is not met according to Courant et al. (1928).

Most of the numerical models used in practice are equipped with some precautions

to stop the calculations when the results tend deviate from logical ranges. Artificial dampers, numerical filters are commonly used methods to control errors if possible. Hence, care must be given to the assessment of numerical model results. Sometimes verification of the parameters for simpler and smaller problems might be necessary. Effects of resolution and other numerical parameters need to be investigated almost in every numerical study. It might not always be possible but it may be better to verify the models with possible alternative numerical models.